การหาค่าเหมาะที่สุดของการผลิตไฮโดรเจนจากเมทานอลโดยใช้กระบวนการรีฟอร์มมิงด้วยไอน้ำ
ที่มีการดูดซับ

นางสาวจันทวรรณ หวังวีระ

วิทยานิพนธ์นี้เป็นส่วนหนึ่งของการศึกษาตามหลักสูตรปริญญาวิศวกรรมศาสตรมหาบัณฑิต
สาขาวิชาวิศวกรรมเคมี ภาควิชาวิศวกรรมเคมี
คณะวิศวกรรมศาสตร์ จุฬาลงกรณ์มหาวิทยาลัย
ปีการศึกษา 2557

OPTIMIZATION OF HYDROGEN PRODUCTION FROM METHANOL USING A
SORPTION-ENHANCED STEAM REFORMING PROCESS

Miss Jantawan Vungvira

A Thesis Submitted in Partial Fulfillment of the Requirements

for the Degree of Master of Engineering Program in Chemical Engineering

Department of Chemical Engineering

Faculty of Engineering

Chulalongkorn University

Academic Year 2014

Thesis Title	OPTIMIZATION OF HYDROGEN PRODUCTION FROM METHANOL USING A SORPTION-ENHANCED STEAM REFORMING PROCESS
By	Miss Jantawan Vungvira
Field of Study	Chemical Engineering
Thesis Advisor	Assistant Professor Amornchai Arpornwichanop, D.Eng.

Accepted by the Faculty of Engineering, Chulalongkorn University in Partial Fulfillment of the Requirements for the Master's Degree

.... Dean of the Faculty of Engineering
(Professor Bundhit Eua-arporn, Ph.D.)

THESIS COMMITTEE

.... Chairman
(Varun Taepaisitphongse, Ph.D.)

.... Thesis Advisor
(Assistant Professor Amornchai Arpornwichanop, D.Eng.)

.... Examiner
(Assistant Professor Soorathep Kheawhom, Ph.D.)

.... External Examiner
(Yaneeporn Patcharavorachot, D.Eng.)

จันทวรรณ หวังวีระ : การหาค่าเหมาะที่สุดของการผลิตไฮโดรเจนจากเมทานอลโดยใช้กระบวนการรีฟอร์มมิงด้วยไอน้ำที่มีการดูดซับ (OPTIMIZATION OF HYDROGEN PRODUCTION FROM METHANOL USING A SORPTION-ENHANCED STEAM REFORMING PROCESS) อ.ที่ปรึกษาวิทยานิพนธ์หลัก: อมรชัย อาภรณ์วิชานพ, 117 หน้า.

การรีฟอร์มมิงด้วยไอน้ำที่มีการดูดซับได้ถูกพิจารณาให้เป็นกระบวนการที่เหมาะสำหรับการผลิตไฮโดรเจน การเติมแคลเซียมออกไซด์ในเครื่องปฏิกรณ์รีฟอร์มเมอร์ทำให้ก๊าซคาร์บอนไดออกไซด์ถูกขจัดออกจากกระบวนการรีฟอร์มมิงด้วยปฏิกิริยาคาร์บอเนชั่น เป็นผลทำให้ผลได้ของไฮโดรเจนมีค่าสูงขึ้น จุดประสงค์ของการศึกษานี้ทำเพื่อหาค่าที่เหมาะที่สุดในการผลิตไฮโดรเจนโดยการใช้กระบวนการรีฟอร์มมิงด้วยไอน้ำที่มีการดูดซับ โดยใช้เมทานอลเป็นสารตั้งต้น การจำลองกระบวนการรีฟอร์มมิงทำโดยโปรแกรมจำลองกระบวนการสำเร็จรูป โดยมีจลหพลศาสตร์ทางเคมีของการรีฟอร์มมิงด้วยเมทานอล ซึ่งประกอบด้วยปฏิกิริยาการรีฟอร์มมิงด้วยไอน้ำของเมทานอล ปฏิกิริยาการสลายตัวของเมทานอล ปฏิกิริยาวอเตอร์ก๊าซชิฟต์ และปฏิกิริยาคาร์บอเนชั่น ถูกใช้ในการอธิบายความเป็นไปของกระบวนการรีฟอร์มมิงด้วยไอน้ำที่มีการดูดซับ การวิเคราะห์ความไวของตัวแปรหลักที่มีผลต่อเครื่องปฏิกรณ์รีฟอร์มเมอร์ด้วยไอน้ำที่มีการดูดซับได้ถูกศึกษา เพื่อใช้ในการวิเคราะห์และประเมินประสิทธิภาพของเครื่องปฏิกรณ์ที่สภาวะการดำเนินการต่างๆ นอกจากนี้ ยังได้มีการหาค่าเหมาะที่สุดสำหรับสภาวะที่ใช้ในการดำเนินกระบวนการรีฟอร์มมิงด้วยไอน้ำที่มีการดูดซับ โดยการหาค่าเหมาะที่สุดนี้จะทำเพื่อให้ได้ปริมาณผลิตภัณฑ์ไฮโดรเจนมากที่สุดภายใต้เงื่อนไขของปริมาณคาร์บอนมอนอกไซด์ในสายผลิตภัณฑ์ไม่เกิน 10 พีพีเอ็ม ผลจากการศึกษาพบว่า ปริมาณเมทานอล 1 โมล จะทำให้ได้ปริมาณไฮโดรเจนสูงสุด 3 โมล เมื่อเครื่องปฏิกรณ์รีฟอร์มเมอร์ถูกดำเนินการที่อุณหภูมิ 350 องศาเซลเซียส และที่ปริมาณสัดส่วนไอน้ำต่อเมทานอลโดยโมลที่ป้อนเข้าเครื่องปฏิกรณ์รีฟอร์มเมอร์ที่ค่า 1.70 การจัดการด้านพลังงานสำหรับกระบวนการรีฟอร์มมิงด้วยไอน้ำที่มีการดูดซับได้ถูกพิจารณาเพื่อเป้าหมายในการลดความต้องการในการใช้พลังงานความร้อนจากภายนอก โดยผลจากการศึกษาพบว่าการจัดการด้านพลังงานความร้อนทำให้สามารถนำความร้อนที่เกิดขึ้นจากกระบวนการกลับมาใช้ในกระบวนการได้ 39.16 เปอร์เซ็นต์ ทำให้มีประสิทธิภาพทางความร้อนของกระบวนการเท่ากับ 75.23 เปอร์เซ็นต์ นอกจากนี้ยังมีการคำนวณกำไรจากกระบวนการผลิตอย่างง่ายโดยอ้างอิงข้อมูลจากกระบวนการรีฟอร์มมิงด้วยไอน้ำเพื่อผลิตไฮโดรเจนที่ดำเนินการอยู่ที่สถานีเติมเชื้อเพลิง โดยผลจากการศึกษาพบว่า การขายไฮโดรเจนที่ผลิตได้จากกระบวนการรีฟอร์มมิงด้วยไอน้ำที่มีการดูดซับเพื่อเป็นเชื้อเพลิงให้กับยานพาหนะสามารถทำกำไรได้ 37.13 เปอร์เซ็นต์ โดยราคาขายของไฮโดรเจนที่ใช้ในการคำนวณเมื่อเปรียบเทียบกับราคาขายของก๊าซโซลีนแล้วมีค่าไม่แตกต่างกันมากนัก

ภาควิชา	วิศวกรรมเคมี	ลายมือชื่อนิสิต	....
สาขาวิชา	วิศวกรรมเคมี	ลายมือชื่อ อ.ที่ปรึกษาหลัก	....
ปีการศึกษา	2557		

5471052021 : MAJOR CHEMICAL ENGINEERING

JANTAWAN VUNGVIRA: OPTIMIZATION OF HYDROGEN PRODUCTION FROM METHANOL USING A SORPTION-ENHANCED STEAM REFORMING PROCESS. ADVISOR: ASST. PROF. AMORNCHAI ARPORNWICHANOP, D.Eng., 117 pp.

A sorption-enhanced steam reforming is considered to be a suitable process for hydrogen production. By adding solid calcium oxide (CaO) to the reformer, carbon dioxide (CO_2) is removed via the carbonation reaction and the yield of hydrogen is improved. The aim of this study was to find the optimal operating condition of the sorption-enhanced steam reforming process using methanol as a hydrogen source. Modeling of the reforming process was done using flowsheet simulator. Kinetics of methanol reforming, methanol steam reforming, methanol decomposition, water gas shift reaction, and carbonation were employed to explain the sorption-enhanced steam reforming. Sensitivity analyses of key parameters of the sorption-enhanced steam reformer were performed to study the performance of the reformer at different operating conditions. Optimization of the sorption-enhanced steam reformer was performed with the objective to find its optimal operating condition by maximizing hydrogen product with the presence of carbon monoxide (CO) less than 10 ppm. It was found that one mole of methanol gave the maximum hydrogen yield of 3 when the reformer was operated at 350 °C and steam-to-methanol molar feed ratio of 1.70. The heat integration of the reforming process was considered to reduce a hot utility requirement and the results showed that useful heat was recovered by 39.16 percents, resulting in the process thermal efficiency of 75.23 percents. A simplified profit estimation and economic analyses were carried out based on on-site reforming at a refuelling station. The estimation showed profit at 37.13 percents based on competitive selling price of hydrogen, comparing to gasoline selling price.

Department:	Chemical Engineering	Student's Signature ....
Field of Study:	Chemical Engineering	Advisor's Signature ....
Academic Year:	2014	

ACKNOWLEDGEMENTS

CONTENTS

LIST OF TABLES

จุฬาลงกรณ์มหาวิทยาลัย
CHULALONGKORN UNIVERSITY

LIST OF FIGURES

LIST OF NOMENCLATURES

$C_{S_i}^{T}$ total surface concentration of site i, $\dfrac{\text{mol}}{\text{m}^2}$

E_i activation energy for rate constant of reaction i, $\dfrac{\text{kJ}}{\text{mol}}$

ΔH_i heat of reaction for formation of surface species i, $\dfrac{\text{kJ}}{\text{mol}}$

$\Delta H_{25^\circ C}$ standard enthalpy change of reaction (at 25 °C), $\dfrac{\text{kJ}}{\text{mol}}$

k_i rate constant for reaction i, $\dfrac{\text{m}^2}{\text{mol s}}$

k_i^{∞} pre-exponential term in Arrhenius expression, $\dfrac{\text{m}^2}{\text{mol s}}$

k_S sorption rate constant, $\dfrac{\text{mol}}{\text{m}^2 \text{s kPa}}$

K_i equilibrium constant of reaction i, dimensionless

n reaction order, dimensionless

P_{CO_2} partial pressure of CO_2, kPa

$P_{CO_2 eq}$ equilibrium partial pressure of CO_2, kPa

r_C carbonation reaction rate, $\dfrac{\text{kmol}}{\text{m}^3 \text{s}}$

r_D rate of methanol decomposition, $\dfrac{\text{mol}}{\text{m}^2 \text{s}}$

r_R rate of methanol steam reforming, $\dfrac{\text{mol}}{\text{m}^2 \text{s}}$

r_S CO_2 sorption reaction rate, $\dfrac{mol}{kgCaO\ s}$

r_W rate of water gas shift reaction, $\dfrac{mol}{m^2\ s}$

R gas constan 8.314 x 10^{-3}, $\dfrac{kJ}{mol\ K}$

S sorbent specific surface area, $\dfrac{m^2}{kg\ CaO}$

ΔS_i entropy of adsorption for species i, $\dfrac{J}{mol\ K}$

η_{CaO} efficiency, dimensionless

α_P solid volume fraction, dimensionless

ρ_P solid density, $\dfrac{kg}{m^3}$

ω_{CaO} mass fraction of CaO, dimensionless

CHAPTER I

INTRODUCTION

Hydrogen is regarded as a clean energy carrier and important chemical in many chemical and petrochemical industries. Furthermore, it can be used as a fuel in fuel cells for power generation. However, because hydrogen is not readily available, it is necessary to produce it from other sources. Many studies on hydrogen production from various non-renewable and renewable fuel sources, such as natural gas, ethanol, methanol and biogas, have been conducted (D.K. Lee at al., 2004: Martinez et al., 2013). Among these various hydrogen sources, methanol has been constantly gaining interest in a small-scale hydrogen production owing to the fact that it can be reformed at low reforming temperature and it also produces high hydrogen concentration with low carbon formation induced by high hydrogen-to-carbon atomic ratio of methanol. Moreover, methanol is in liquid state at atmospheric condition leading to convenient and safe transportation and storage (Martinez et al., 2013).

There are several technologies for hydrogen production, for instance, partial oxidation, autothermal reforming, and steam reforming (Pajaie et al., 2012; Peng, 2003). Steam reforming is a thermal process which is carried out over a nickel-based catalyst. The process involves reacting methane or light hydrocarbons with steam by applying heat (Peng, 2003). Partial oxidation is another thermal process, which mainly deals with heavier petroleum feedstocks. Fuel, steam and air are reacted with or without a catalyst, depending on the type of feedstock and process chosen (Peng, 2003). Partial oxidation process involves a strong exothermic reaction which can give a fast response for an automotive system comparing to steam reforming process.

Nevertheless, the purity of hydrogen product by the partial oxidation process of methanol is in a low range; theoretical hydrogen concentration (percentage of moles of hydrogen produced per moles of total gas product by the stoichiometry) of 66% is achieved with using pure oxygen, whereas theoretical hydrogen concentration of 41% is achieved with using air instead of pure oxygen (Pajaie et al., 2012). Autothermal reforming is a process which combines steam reforming and partial oxidation in a single unit (Peng, 2003). Fuel, steam and air are reacted in the autothermal reformer over the mixed catalyst which supports both steam reforming reaction and partial oxidation reaction (Peng, 2003). Heat generated by the exothermic reaction of partial oxidation supplies to the endothermic reaction of steam reforming. Hence, external heat source is not required for this process. However, the estimated hydrogen concentration for the autothermal reforming process of methanol is only 40-50% of total gas product on molar dry basis . Steam reforming is acknowledged as a highly efficient hydrogen production process. As reported by Pajaie et al. (2012), the steam reforming of methanol can yield up to 75% of hydrogen concentration in total gas product on molar dry basis. The same range of high hydrogen concentration by the steam reforming of methanol is also reported by Katiyar et al. (2013) at 70-80% of total gas product on molar dry basis. Despite the fact that steam reforming is a productive process for hydrogen production, there are some windows for improvement to eliminate the disadvantages of this process.

One of the most serious obstacles to the operation of the steam reforming process is the thermodynamic equilibrium of reversible reforming reactions. As reported by Martinez et al. (2013), reverse water gas shift reaction occurred in hydrogen-rich environment at high steam reactant feed rate and low reforming

temperature. For a conventional steam reforming of methane, high reaction temperature is required to achieve complete fuel conversion; however, such operating conditions favor the formation of carbon, which leads to the deactivation of the reforming catalysts (Peng, 2003). In general, the hydrogen-rich gas derived from the reforming process of methanol is composed of H_2, CO, CO_2 and CH_4. To achieve high purity of hydrogen product, the conventional steam reforming process is integrated with other gas cleaning units, such as water gas shift reactor and preferential oxidation (PROX) reactor (Choi & Stenger, 2005) which leads to more complex hydrogen production and purification processes. Therefore, several modifications of the reforming system have been invented to minimize the complexity of the system and to enhance the hydrogen production (Katiyar et al., 2013; Mahishi et al., 2008; Martinez et al., 2013; Peng, 2003).

The coupling of reaction and separation systems is an interesting approach to improve the performance of a fuel processor and to reduce its complexity. Membrane enhanced steam reforming is an example of a well-developed technology for hydrogen production. With the use of membrane, hydrogen is continually removed from the reaction zone during the reforming of fuel; consequently, the equilibrium-limited reforming reaction is shifted forward to the hydrogen product side. The disadvantage of this membrane application is the damage of membrane due to feed impurities. Hence, the feed gas needs to be purified before entering the membrane reactor (Peng, 2003). In addition, a high cost of the membrane production for industrial uses is still the limitation for the usability of membrane (Nijmeijer, 1999).

Alternatively, a sorption-enhanced steam reforming process has been proposed to minimize the complexity of the fuel processor and to enhance the hydrogen

production (Katiyar et al., 2013; Mahishi et al., 2008; Martinez et al., 2013; Peng, 2003). The sorption-enhanced steam reformer can be operated by a packed bed reactor or a fluidized bed reactor containing calcium oxide (CaO) sorbent and the reforming catalysts. CaO sorbent is added to the steam reformer to adsorb generated CO_2 via a carbonation reaction. The removal of CO_2 causes the reforming equilibrium to shift toward the hydrogen production (Martinez et al., 2013). Hence, high purity of hydrogen product is achieved in a single reformer without any further purification unit. In case of the steam reforming of methane, the use of CaO sorbent can lower the operating temperatures compared to that required for the conventional reforming process (Ding & Alpay, 2000). Although the sorption-enhanced steam reforming is theoretically in favor of hydrogen production, there is still a suspicion about a low performance in terms of high energy consumption due to a regeneration unit of a spent CaO sorbent.

As demonstrated by the previous reviews of several technologies for hydrogen production, the selection of various components in the fuel processor significantly affects the efficiency and the cost of the fuel processor. To achieve a high performance of the sorption-enhanced steam reforming, optimization of the operating conditions could be a solution. There are limited works that deal with the optimization of the sorption-enhanced steam methanol reforming .

The objective of this study was to improve the performance of the sorption-enhanced steam reforming process for hydrogen production. Methanol was used as the fuel supply owing to its low reforming temperature and high hydrogen-to-carbon atomic ratio. The sensitivity analyses of primary design parameters on the sorption-enhanced steam methanol reforming process were performed first. The optimization

of such process was then carried out to determine their optimal values. The amount of heat required was also investigated, then the heat integration based on a pinch analysis was employed to figure out the possibility of heat recovery within the process. Regarding the heat recovery operation, hot utilities requirement became lower resulting in the reduction of the production cost. Finally, an economic analysis of the sorption-enhanced steam methanol reforming process was conducted to show the possibility of the implementation in the future.

CHAPTER II

LITERATURE REVIEW

A review of literature related to this work was performed in order to gain the background knowledge of the research scope and to discover interesting issues and problem in the area that had been identified by other researchers. Moreover, the review of literature is a procedure for data collection in terms of research methodology, theory, and basic assumption used in this research. There were many past researches concerning chemical processes for hydrogen production, in which the details are presented in the following sections. To provide a better understanding of the past researches and this work, theory related to the research scope are explained in CHAPTER III.

2.1 Hydrogen production by conventional steam reforming process

Hydrogen production by a conventional steam reforming process has been continuously studied in various aspects. Choi and Stenger (2005) performed the experiments to solve for the kinetic rate expressions of the conventional steam reforming of methanol. Then, a simple process for hydrogen production was simulated by MATLAB with a plug flow reactor model using their own kinetic rate expressions. The process simulation of hydrogen production was conducted to study the effect of process parameters on product distribution and to perform the optimization to achieve the optimal operating conditions. Three reactors were conducted in the simulation as follow: steam reformer, water gas shift reactor and preferential oxidation (PROX) reactor. Results from the optimizations showed that the

suitable steam reforming temperature and water gas shift reaction temperature ranges based on a commercial $Cu/ZnO/Al_2O_3$ catalyst were about 300-350 °C and 220 °C, respectively. For the last PROX reactor, the optimal operating temperature was 250 °C. The kinetic rate expressions for the steam reforming of methanol were reported by several authors (J. K. Lee et al., 2004; Peppley et al., 1999; Tesser et al., 2009). However, the kinetic model developed by Peppley et al. (1999) appears to be the most widely referenced and extensively used for the steam reforming of methanol (Li et al., 2012; Lotric & Hocevar, 2012). Details for the kinetic models of the steam reforming of methanol are described in CHAPTER III.

2.2   Hydrogen production by sorption-enhanced steam reforming process

The sorption-enhanced steam reforming is the combination of reforming reactions and carbonation reaction. All these reactions occurred in a single sorption-enhanced steam reformer. Details for the kinetic model of the carbonation reaction are illustrated in CHAPTER III.

The sorption-enhanced steam reforming of methanol is lacking information regarding kinetic-based simulation; available literatures simulated in the same manner have been found to use other type of raw materials (Feole, 2013; Johnson et al., 2006; D. K. Lee et al., 2004; Sanchez et al., 2012; Yunus, Ahmad, Inayat, & Yusup, 2010). Sanchez et al. (2012) compared the sorption-enhanced steam reforming of methane based on a circulating fluidized bed reactor with experimental result; the kinetic rates of methane steam reforming and carbonation, based on dolomite with intrinsic rate constant of the $CaO-CO_2$ reaction, used were developed by Xu and Froment (1989) and Sun et al. (2008) respectively.

Martinez et al. (2013) performed the thermodynamic modeling of sorption-enhanced steam reforming of light alcohols, ethanol and methanol, to determine the operating conditions for production of high purity of hydrogen. The reforming systems were simulated in the temperature range between 300-600 °C and S/C feed ratio (steam-to-methanol molar feed ratio) ranging from 1 to 6. Referring to the sorption-enhanced steam reforming of methanol, the results showed that by using CaO to capture CO_2, it could enhance the hydrogen yield (moles of hydrogen produced at equilibrium per moles of methanol fed to the system) as it was about 7% higher in comparison with the conventional steam reforming, while hydrogen concentration changed from 73% to 98% of total gas product on molar dry basis at the temperature of 600 °C and S/C feed ratio of 6. With minimum reforming temperature and S/C feed ratio based on the scope of the study, hydrogen yield was achieved at 2.9 at the temperature of 300 °C and S/C feed ratio of 4. However, S/C feed ratios in lower region, between 2 and 3 were not included in this study. In the same way, hydrogen concentration could be attained at 99.6% of total gas product on molar dry basis in the temperature range of 300-500 °C and S/C feed ratio of 4. Hydrogen concentration in total gas product of 99.8% on molar dry basis was obtained in a higher S/C feed ratio of 5 in the temperature range of 300-400 °C.

In general, the study of product distribution at equilibrium can be performed by the thermodynamic equilibrium calculation and two approaches are proposed for this method: stoichiometric approach and non-stoichiometric approach. For non-stoichiometric approach, the equilibrium compositions of products are derived by the direct minimization of Gibbs free energy. For stoichiometric approach, the system is

described by stoichiometric reactions and their equilibrium constants (Katiyar et al., 2013).

Thermodynamic analyses by stoichiometric method for the conventional and sorption-enhanced steam reforming of methanol were investigated by Katiyar et al. (2013). Under the conventional steam reforming with CO, CO_2, and H_2 as desired products, methanol conversion was completed in the temperature range of 177-227 °C, pressure of 1 atm and steam-to-methanol molar feed ratio (S/C feed ratio) of 1-1.5. Hydrogen yields (moles of hydrogen produced at equilibrium per moles of methanol fed to the system) were in the range of 2.86-2.98. Hydrogen concentrations in total gas product were 74.1-74.9% on molar dry basis. With CO, CO_2, H_2, and dimethyl ether (DME) as desired products, hydrogen yield and CO amount were investigated at different temperatures and S/C feed ratios. Results showed that the increase of S/C feed ratio suppressed the rates of methanol decomposition and methanol dehydration and enhanced the hydrogen production through the methanol reforming. At high temperature, high CO amount was achieved at low S/C feed ratio (S/C feed ratio <1) due to the predominance of methanol decomposition over methanol steam reforming. The reduction of CO was found at low temperature and high S/C feed ratio as the water gas shift reaction was thermodynamically favorable at low temperature. With an introduction of excess steam, water gas shift reaction caused an extreme reduction of CO and brought about more CO_2 and hydrogen production. However, very small amount of DME was presented at temperature above 177 °C and S/C feed ratio of 1.5. Regarding the study of sorption-enhanced steam reforming of methanol based on the desired products of CO, CO_2, and H_2 with an additional formation of carbon species, hydrogen yield was reported at 2.6 with

relatively complete CO removal. From the study, the shift of equilibrium which favored hydrogen production occurred when CO_2 was removed by CaO sorbent since the removal helped promote water gas shift reaction.

Both fixed bed and fluidized bed have been used to represent the sorption-enhanced steam reforming system (Johnson et al., 2006; Vicente et al.). The sorption-enhanced steam reforming can provide a very high purity of hydrogen in the proper conditions. Li et al. (2012) performed a preliminary study of hydrogen production using adsorption enhanced reforming (AER) of methanol in a packed bed reactor. The results showed that high hydrogen production could be accomplished in a single reformer. Chao et al. (2011) performed the simulation of sorption-enhanced steam reforming of methane based on non-thermodynamic equilibrium calculation. The simulation was performed based on a set of stoichiometric reactions and their kinetic rate expressions. Results showed that the hydrogen concentration in total product gas at the outlet of the sorption-enhanced steam reformer was achieved at 98.75% on molar dry basis at the reforming temperature of 575 °C and S/C feed ratio (steam-to-methane feed molar ratio) of 5.

2.3   Kinetic model of CaO-CO_2 reaction (Carbonation reaction)

Several kinetic models of CaO-CO_2 reaction by CaO-based sorbent have been studied and reviewed in many literatures. Mostafavi et al. (2013) studied the thermodynamic and kinetic simulation of the CO_2 capture based on two calcium-based sorbents, Imasco dolomite and Cadomin limestone, using Aspen Plus. The elemental analyses of the sorbents showed that CaO composition in Cadomin limestone and Imasco dolomite were 54.30% by weight and 36.97% by weight,

respectively. The intrinsic rate constants were applied for the kinetic simulation. The experiments for CO_2 capture were conducted to validate the simulation results. Results from modeling and experimental data were in a good agreement and the maximum conversion of CaO was achieved at 650 °C. From the study of the initial carbonation reaction rate, higher CaO active sites available in calcium-based sorbent resulted in better accessibility of CO_2 molecules to the CaO molecules and high reaction rate. Thus, the reaction rate for Cadomin limestone was higher than that obtained by Imasco dolomite due to the higher amount of CaO at the surface. Sun et al. (2008) studied the intrinsic rate constant of the $CaO-CO_2$ reaction for Strassburg limestone and Arctic dolomite using an atmospheric thermogravimetric analyzer (ATGA) and a pressurized thermogravimetric analyzer (PTGA). CaO composition in Strassburg limestone and Arctic dolomite were 53.70% by weight and 30.51% by weight, respectively. The intrinsic rate was developed using a grain model which is the model that represents the pattern of carbonation reaction mechanism on surface into limestone particle. As seen in CHAPTER III, the reaction order of carbonation reaction was found to vary depending on CO_2 partial pressure. The reaction order of carbonation reaction was first-order when the driving force of reaction in terms of CO_2 partial pressure was less than 10 kPa. For the higher driving force, zero-order was used to explain the carbonation reaction. The activation energies for Strassburg limestone and Arctic dolomite were 29 ± 4 kJ/mol and 24 ± 6 kJ/mol, respectively. The structural difference between the two sorbents was speculated to influence the variance in the activation energies.

2.4   Optimization of hydrogen production process

The optimization of hydrogen production from methane with additional CO_2 reformer was studied by Wu et al. (2012). CO_2 reformer was added into the conventional steam reforming system by adding between steam methane reformer and high temperature shift converter. Maximization of hydrogen production and minimization of CO_2 emission were analyzed as the objective functions. The decision variables for the optimization included steam-to-methane molar feed ratio, inlet temperature of steam methane reformer, inlet temperature of CO_2 reformer, and inlet temperature of high temperature shift converter. The sensitivity analyses of the decision variables were performed in order to study the effect of these variables on the production. The Multi-Objective Optimization Problem (MOO) was solved by Non-Dominated Sorting Genetic Algorithm-II (NSGA-II). Finally, the heat recovery was applied on the system and validated by Aspen Hysys simulator.

Choi and Stenger (2005) used MATLAB to determine the optimal conditions of hydrogen production by the conventional steam reforming of methanol. The optimal reactor size, temperature, amount of water added to each reactor, and the air-to-CO feed ratio to PROX reactor were verified to maximize economic profit.

The optimization of conventional steam reforming is common and readily available as literatures whereas the optimization for the sorption-enhanced steam reforming is rare, as the process is still under development (Tzanetis et al., 2012).

2.5   Reduction of heat consumption for hydrogen production process

A minimization of heat consumption for hydrogen production process has been proposed via heat integration method. Posada and Manousiouthakis (2005)

performed heat and power integration studies for the hydrogen production process based on the conventional steam reforming of methane. To minimize hot utility and cold utility costs, the optimal integrations of heat exchanger by hot streams and cold streams were carried out by a pinch analysis. According to the heat integration of hot streams and cold streams, hot utility was not required in the reforming process leading to the reduction in utility cost of 36%, and the reduction in CO_2 emission (kilograms of CO_2 per kilograms of hydrogen) of 6.5%.

Wu et al. (2012) proposed the hydrogen production process with CO_2 reformer-aided steam methane reforming. The process optimization was performed to determine the feasible operating conditions. Finally, a simple heat integration design was implemented to the process to reduce energy consumption.
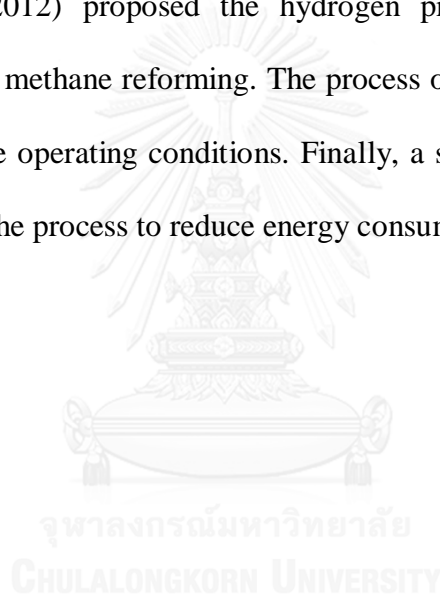
CHAPTER III

THEORY

This chapter was provided to summarize theory and basic ideas with respect to the research topic. The first section describes the importance of methanol in hydrogen production application by steam reforming process. This section shows the advantage and motivation of using methanol for steam reforming process. In the second section, general steam reforming reactors used in chemical and petrochemical industries are introduced to illustrate their characteristic and application. Based on this research, the studies of process parameters for steam reforming of methanol and optimization were performed by a software package, "Aspen Plus". The simulations of main reforming reactors were based on reaction kinetic rates using a plug flow reactor model. Other reactors provided in the processes were simulated with a stoichiometric reactor. Hence, the third section is provided to describe reaction mechanisms and rate expressions used in the simulation. Details of parameters used in the rate expressions are presented in these sections. The plug flow reactor model, the stoichiometric reactor model, and heat balance equations are summarized in the fourth section to explain the mathematic equations used in this work. The fifth section provides basic knowledge about optimization method used in this work namely "Sequential Quadratic Programming". In the last section, overall concept and procedure in heat integration and heat exchanger network design are simplified for introduction.

3.1 Methanol

Methanol is an oxygenated hydrocarbon with the formula of CH_3OH. Methanol is an alternative source that has been used for hydrogen production. It is generally produced by several raw materials, such as natural gas, coals, and biomass (Martinez et al., 2013; S. Sa et al., 2009). The structural formula of methanol is illustrated in Fig. 1 (Laumer, 2006). The properties of methanol relative to other fuels are presented in Table 1 (Alternative Fuels Data Center. U.S. Department of Energy, 2014).
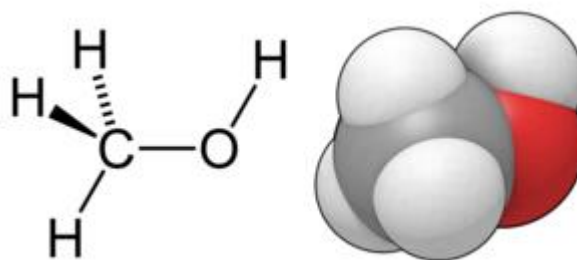
Fig. 1   Structural formula of methanol (Laumer, 2006)

Table 1   Fuel properties of methanol and others (Alternative Fuels Data Center. U.S. Department of Energy, 2014)

Properties	Methanol	Ethanol	Gasoline	CNG*	Hydrogen
Chemical structure	CH_3OH	CH_3CH_2OH	C_4 to C_{12}	CH_4 (83-99% by weight), C_2H_6 (1-13% by weight)	H_2
Fuel material (feedstocks)	Natural gas, coal, woody biomass	Corn, grain, agriculture waste (cellulose)	Crude oil	Underground reserves	Natural gas, methanol, electrolysis of water

*CNG is Compressed Natural Gas.

Table 1   Fuel properties of methanol and others (Alternative Fuels Data Center. U.S. Department of Energy, 2014) (continued)

Properties	Methanol	Ethanol	Gasoline	CNG*	Hydrogen
Low heating value	57,250 Btu/gal (g)	76,330 Btu/gal E100 (g)	116,090 Btu/gal (g)	20,268 Btu/ lb (g)	61,013 Btu/ lb (g)
Physical state	Liquid	Liquid	Liquid	Compressed gas	Compressed gas or liquid
Flash point	11.1 °C	12.8 °C	-42.8 °C	-184.4 °C	N/A
Autoignition temperature	480.6 °C	422.8 °C	257.2 °C	540.0 °C	565.6-582.2 °C

*CNG is Compressed Natural Gas.

According to many researches concerning hydrogen production, methanol is popular as raw material for small stationary reformers in hydrogen production. There are many advantages of methanol in terms of hydrogen production comparing to other fuels. The benefits of methanol include:

a) Lower production costs compared with other alternative fuels (Alternative Fuels Data Center. U.S. Department of Energy, 2014).

b) Better energy security since methanol can be produced from various carbon-based feedstock (Alternative Fuels Data Center. U.S. Department of Energy, 2014), for instance, natural gas, coals, and biomass.

c) Methanol has high hydrogen to carbon atomic ratio. Hence, methanol conversion theoretically leads to high hydrogen concentration with low carbon formation (Martinez et al., 2013).

d) Lower reforming temperature of oxygenated hydrocarbons, e.g., ethanol, methanol (which is around 200-300 °C) compared with reforming temperature of non-oxygenated hydrocarbons, i.e., methane (Martinez et al., 2013; S. Sa et al., 2009).

e) Methanol is liquid at the atmospheric condition and has lower flammability compared with gasoline (Alternative Fuels Data Center. U.S. Department of Energy, 2014), leading to convenient and safe for transportation and storage in any vehicle or stationary/mobile equipment.

3.2   Steam reforming reactors

A competitive and preferred process, wildly used in hydrogen production is a steam reforming of liquid or gas hydrocarbons. Steam reforming is employed in many different types of reactors. The main reactor technologies are summarized as follow:

3.2.1   Fired steam reformer

Fired steam reformer is the most common design for the steam reforming reactor. Several tubes filled with catalysts are placed in rows inside a firebox. Gas feedstock is burned inside the tubes via burners installed at the firebox wall. More than one arrangement for the burners can be designed. The burners can be located on the floor, on the roof, on the wall terraces, or on the walls (side fired) as illustrated in Fig. 2 (Wesenberg, 2006).

.
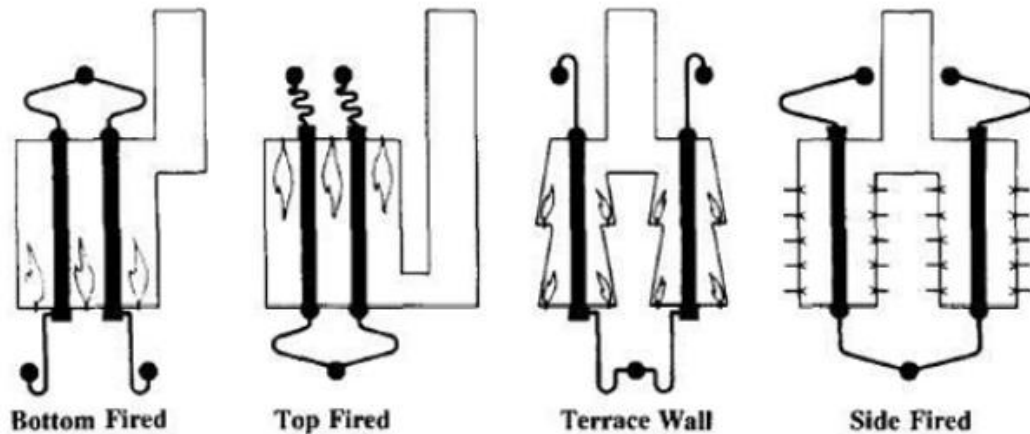
Fig. 2   Fired steam reformer with different burner arrangements (Wesenberg, 2006)

There is a heat recovery process on the flue gas stream leaving the fire box which is utilized in a preheater resulting in high overall thermal efficiency of the fired duty at 90-97%, although direct firing of the burners on to the reactor tubes has only about 50% efficiency (Wesenberg, 2006).

The fired steam reformer is used for a conversion of light hydrocarbon feedstock to synthesis gas, hydrogen, carbon monoxide, town gas, etc. In chemical and petro-chemical industries, the fired steam reformer is applied in productions of ammonia synthesis gas, methanol synthesis gas, hydrogen, etc. (Dybkjaer, 1995).

3.2.2   Heat exchange reformer

Heat supply for reforming reaction employed in this type of steam reformer is provided by heat exchanged by the heating gas. The heat exchange steam reformer is suitable for hydrogen production in fuel cell plants owing to its advantageous compactness, high efficiency (Dybkjaer, 1995), and less expensive (Wesenberg, 2006) comparing to the fired steam reformer. The available heat exchange reformer

for fuel cell is operated at the capacity of 504,000 Nm^3/h (normal cubic meter per hour) of hydrogen in low pressure condition. In higher pressure applications and for larger capacities, "convection reformer", which is an improved design of this type of reformer, is used in place of the conventional one. The demonstration of this unit in a full-scale process has been operated by Topsoe in Houston, Texas, USA (Dybkjaer, 1995). Although the convection reformers are still in a developing stage, it has been commercially used in large scale processes of ammonia production and hydrogen production (Wesenberg, 2006).

The simplest geometry for the heat exchange steam reformer/convection reformer is a counter-current heat exchanger. Process gas enters the reactor tubes at the top while the heating gas enters shell side at the bottom (Wesenberg, 2006). The steam reforming process in reactor tubes is induced by the heat which is transferred from the heating gas stream in the shell side.

3.3   Kinetic rate expressions of steam methanol reforming (SMR) and CaO-CO_2 reaction

The process simulations of the conventional steam methanol reforming (SMR) and the sorption-enhanced steam methanol reforming (SE-SMR) in this work were performed based on reaction kinetic rates. In this work, the conventional steam methanol reforming process was based on the methanol reforming reactions on $Cu/ZnO/Al_2O_3$ catalyst, i.e., methanol steam reforming, methanol decomposition, and water gas shift reaction (Eqs. (1)-(3)). The sorption-enhanced steam methanol reforming process was based on the methanol reforming reactions as mentioned (Eqs. (1)-(3)) and CaO-CO_2 reaction (Eq. (9)). To simulate both steam reforming processes,

the reaction kinetic rates were input through the built-in reactions models in Aspen Plus software. Details of kinetic parameters of all those mentioned reactions are presented as follow.

3.3.1 Kinetic rate expressions of steam methanol reforming (SMR)

To describe and investigate the reaction rates as the functions of temperature and chemical concentration in methanol steam reformer, kinetic rate expressions proposed by Peppley et al. (1999) were used for kinetic models applied in the plug flow reactor. The kinetic rate expressions proposed by Peppley et al. (1999) are well known and used in many literatures related to the steam methanol reforming (SMR) using $Cu/ZnO/Al_2O_3$ catalyst (Ghasemzadeh et al., 2013; Lotric & Hocevar, 2012; Purnama, 2003 ; S. T. Sa, 2011; Telotte et al., 2008; Vadlamudi & Palanki, 2011). Three reactions involved in the steam reforming of methanol include methanol decomposition (Eq. (1)), methanol steam reforming (Eq. (2)) and water gas shift reaction (Eq. (3)):

$$CH_3OH \leftrightarrow CO + 2H_2, \Delta H_{25°C} = 90.64 \text{ kJ mol}^{-1} \tag{1}$$

$$CH_3OH + H_2O \leftrightarrow CO_2 + 3H_2, \Delta H_{25°C} = 49.47 \text{ kJ mol}^{-1} \tag{2}$$

$$CO + H_2O \leftrightarrow CO_2 + H_2, \Delta H_{25°C} = -41.17 \text{ kJ mol}^{-1} \tag{3}$$
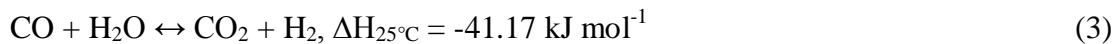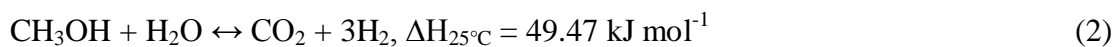
Details of the kinetic rate expressions available in methanol steam reformer are shown in Eqs. (4)-(6):

Methanol decomposition:

$$r_D = \frac{k_D K^*_{CH_3O^{(2)}}(p_{CH_3OH}/p_{H_2}^{1/2})(1 - p_{H_2}^2 p_{CO}/k_D p_{CH_3OH})C^T_{S_2} C^T_{S_{2a}}}{(1 + K^*_{CH_3O^{(2)}}(p_{CH_3OH}/p_{H_2}^{1/2}) + K^*_{OH^{(2)}}(p_{H_2O}/p_{H_2}^{1/2}))(1 + K^{1/2}_{H^{(2a)}}p_{H_2}^{1/2})} \quad \frac{\text{mol}}{\text{m}^2 \text{ s}} \tag{4}$$

Methanol steam reforming:

$$r_R = \frac{k_R K^*_{CH_3O^{(1)}}(p_{CH_3OH}/p_{H_2}^{1/2})(1 - p_{H_2}^3 p_{CO_2}/k_R p_{CH_3OH} p_{H_2O})C^T_{S_1}C^T_{S_{1a}}}{(1 + K^*_{CH_3O^{(1)}}(p_{CH_3OH}/p_{H_2}^{1/2}) + K^*_{HCOO^{(1)}}p_{CO_2}p_{H_2}^{1/2} + K^*_{OH^{(1)}}(p_{H_2O}/p_{H_2}^{1/2}))(1 + K_{H^{(1a)}}^{1/2}p_{H_2}^{1/2})} \quad \frac{mol}{m^2 \ s} \tag{5}$$

Water gas shift reaction:

$$r_W = \frac{k_W K^*_{OH^{(1)}}(p_{CO}p_{H_2O}/p_{H_2}^{1/2})(1 - p_{H_2}p_{CO_2}/k_W p_{CO}p_{H_2O})C^{T^2}_{S_1}}{(1 + K^*_{CH_3O^{(1)}}(p_{CH_3OH}/p_{H_2}^{1/2}) + K^*_{HCOO^{(1)}}p_{CO_2}p_{H_2}^{1/2} + K^*_{OH^{(1)}}(p_{H_2O}/p_{H_2}^{1/2}))^2} \quad \frac{mol}{m^2 \ s} \tag{6}$$

The temperature dependence of rate constants (k_i) and equilibrium constants (K_i) are determined by Arrhenius equation and Van't Hoff equation as expressed in Eqs. (7)-(8). Total site concentrations are 7.5 x 10^{-6} mol/m^2 for Type 1 (C^T_{S1}) and Type 2 (C^T_{S2}) and 1.5 x 10^{-5} mol/m^2 for Type 1a (C^T_{S1a}) and Type 2a (C^T_{S2a}). Parameters for kinetic rate expressions of steam methanol reforming on Cu/ZnO/Al$_2$O$_3$ catalyst are presented in Table 2 .

Arrhenius equation:

$$k_i = k_i^\infty \exp\left(\frac{E_i}{RT}\right) \tag{7}$$

Van't Hoff equation:

$$K_i = \exp\left(\frac{\Delta S_i}{R} - \frac{\Delta H_i}{RT}\right) \tag{8}$$

Table 2   Parameters for kinetic rate expressions of steam methanol reforming on $Cu/ZnO/Al_2O_3$ catalyst (Peppley et al., 1999)

Rate constant or equilibrium constant	ΔS_i (J mol^{-1}K^{-1}) or k^∞_i (m^2 mol^{-1} s^{-1})	ΔH_i or E_i (kJ mol^{-1})
k_R (m^2 mol^{-1} s^{-1})	7.4 x 10^{14}	102.8
$K^*_{CH3O}{}^{(1)}$ (bar$^{-0.5}$)	-41.8	-20.0
$K^*_{OH}{}^{(1)}$ (bar$^{-0.5}$)	-44.5	-20.0
$K_H{}^{(1a)}$ (bar$^{-0.5}$)	-100.8	-50.0
$K^*_{HCOO}{}^{(1)}$ (bar$^{-1.5}$)	179.2	100.0
k_D (m^2 s^{-1} mol^{-1})	3.8 x 10^{20}	170.8
$K^*_{CH3O}{}^{(2)}$ (bar$^{-0.5}$)	30.0	-20.0
$K^*_{OH}{}^{(2)}$ (bar$^{-0.5}$)	30.0	-20.0
$K_H{}^{(2a)}$ (bar$^{-0.5}$)	-46.2	-50.0
k_W (m^2 s^{-1} mol^{-1})	5.9 x 10^{13}	87.6

3.3.2 Kinetic rate expressions of CaO-CO$_2$ reaction

The adsorption of CO_2 by calcium sorbents have been applied in hydrogen production. CaO sorbent reacts with CO_2 to produce $CaCO_3$ as the main product. The reaction between CaO-CO_2 is called "Carbonation". The carbonation can be occurred in various ranges of temperature. Martinez et al. (2013) studied the absorption enhanced reforming of light alcohols by CaO sorbent; the operating temperature was studied in the range of 300-800 °C. For CO_2 scavenging system, CaO can adsorb CO_2 and reduce CO_2 to very low concentration in the moderate temperature of 450-700 °C . Spent CaO or $CaCO_3$ is thermally regenerated later by "Calcination". At calcination conditions, $CaCO_3$ will release CO_2 and become CaO. The calcination temperature is higher than 850 °C (Sivalingam, 2012). Calcium sorbents were found in two forms in nature, limestone, consisting mainly of $CaCO_3$ and dolomite, a combination of calcium and magnesium carbonates ($CaCO_3.MgCO_3$) (Sivalingam, 2012). The

efficiency of sorbent reactivity depends on three parameters: geographical origin of the sorbent (source of the sorbent), calcination temperature, and the cycle of capture and release (Sivalingam, 2012). Arctic dolomite was selected for use in this work since the information about the reaction rate of carbonation was clearly indicated in the literatures (Sanchez et al., 2012; Sun et al., 2008). Chemical analyses for the Arctic dolomite are illustrated in Table 3.

Table 3   Chemical analyses for the Arctic dolomite (% by wt) (Sun et al., 2008)

Sorbent	SiO_2	Al_2O_3	Fe_2O_3	MgO	CaO	Na_2O	K_2O	LOI
Arctic dolomite	2.12	0.17	1.30	21.25	30.51	0.15	0.04	44.4

The reaction rate for carbonation by the CaO-based sorbent is a function of CO_2 partial pressure driving force or P_{CO2}-P_{CO2eq}. In this study, results from the sensitivity analyses showed that the CO_2 partial pressure driving forces were less than 10 kPa in every condition. The reaction mechanisms of carbonation (forward reaction) and calcination (reverse reaction) are presented in Eq. (9):

$$CaO + CO_2 \leftrightarrow CaCO_3, \Delta H_{25°C} = -182.10 \text{ kJ mol}^{-1} \tag{9}$$

The reaction rate of carbonation of Arctic dolomite is presented in Eqs. (10)-(14) . Parameters and other constants are indicated in Table 4.

Carbonation (Arctic dolomite):

$$r_C = 10^{-3} \eta_{CaO} \alpha_P \rho_P \omega_{CaO} r_S \quad \frac{kmol}{m^3 s} \tag{10}$$

$$r_S = k_S (P_{CO_2} - P_{CO_{2eq}})^n S \quad \frac{mol}{kg_{CaO} s} \tag{11}$$

$$k_S = 1.04 \times 10^{-4} \exp\left(\frac{-24 \text{ kJ/mol}}{RT}\right) \quad \frac{\text{mol}}{\text{m}^2 \text{s kPa}} \tag{12}$$

$$P_{CO_2} - P_{CO_2eq} \begin{cases} \leq 10 \text{ kPa} \quad n = 1; \quad k_S = 1.04 \times 10^{-4} \exp\left(\frac{-24 \text{ kJ/mol}}{RT}\right) \quad \frac{\text{mol}}{\text{m}^2 \text{s kPa}} \\ \\ \\ > 10 \text{ kPa} \quad n = 0; \quad k_S = 1.04 \times 10^{-3} \exp\left(\frac{-24 \text{ kJ/mol}}{RT}\right) \quad \frac{\text{mol}}{\text{m}^2 \text{s}} \end{cases} \tag{13}$$

$$P_{CO2eq} = 10^{\frac{-8308}{T}+9.079} \quad \text{kPa} \tag{14}$$

Table 4   Parameters and constants for reaction rate of carbonation (Arctic dolomite)

Parameters and constants
$\eta_{CaO} = 1*$
$\alpha_P = 0.13\text{-}0.47**$
$\rho_P = 1500 \text{ kg m}^{-3}$ (Sanchez et al., 2012)
$\omega_{CaO} = 0.3051$ (as presented in Table 3, Sun et al, 2008)
$S = 31 \text{ m}^2 \text{ gCaO}^{-1}$ (Sun et al., 2008)

* The efficiency of CaO was assumed at 100% for this work.
** Volume fraction of CaO sorbent per solid volume in reactor is a variable process parameter. For this work, this parameter was varied in the range of 0.13-0.47 to investigate and find out the optimal amount of CaO sorbent used in the reactor.

3.4   Plug flow reactor model, RStoic reactor model, and heat balance

In this work, the conventional steam methanol reforming (SMR) process and the sorption-enhanced steam methanol reforming (SE-SMR) process were simulated using Aspen Plus software. The main steam methanol reforming reactors from two mentioned processes were simulated using RPlug reactor. RPlug reactor is conducted

by RPlug model which is the module provided in Aspen Plus software. RPlug rigorously models plug flow reactor and handles rate-based kinetic reactions only (Aspen Plus Version 8.2., 2014). The kinetic rate expressions used in this work are described in Section 3.3. The RPlug model represents an ideal plug flow reactor with one or more phases (Aspen Plus Version 8.2., 2014). The model assumes perfect radial mixing within and between the phases, phase equilibrium, and no-slip conditions between the phases (e.g., the phases all have the same residence time) (Aspen Plus Version 8.2., 2014). Other reactors (e.g., water gas shift reactor, preferential oxidation reactor, regeneration unit) provided in the simulations were based on RStoic reactor as illustrated in CHAPTER IV. Details of both reactor models and heat balance are summarized as follow.

3.4.1 Plug flow reactor model

The model of a steady state plug flow reactor is explained by equations summarized by Levenspiel (1999). In a plug flow reactor, the composition of the fluid varied from point to point along a flow path. Therefore, the material balance for a reaction component is made for a differential element of volume dV. Thus, the material balance for reactant i becomes

$$\text{input} = \text{output} + \text{disappearance by reaction} + \text{accumulation} \qquad (15)$$

$$0$$

Terms for volume dV, referring to Fig. 3 are

input of i, moles/time $= F_i$

output of i, moles/time $= F_i + dF_i$

disappearance of i by reaction, moles/time $= (-r_i)dV$

$$= \left(\frac{\text{moles i reacting}}{\text{(time)(volume of fluid)}} \right) (\text{volume of element})$$

Introducing these three terms in Eq. (15), we obtain

$$F_i = (F_i + dF_i) + (-r_i)dV$$

Replace $dF_i = d[F_{i0}(1-X_i)] = -F_{i0}dX_i$, we obtain

$$F_{i0}dX_i = (-r_i)dV \tag{16}$$
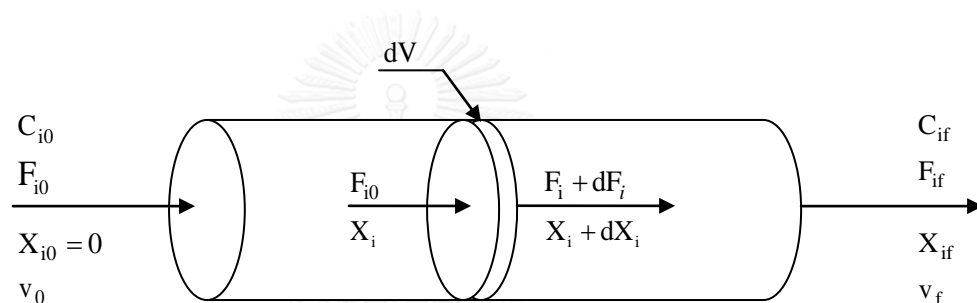
Fig. 3   Notation for a plug flow reactor

Eq. (16) is integrated to represent a whole reactor. r_i depends on concentration or conversion of materials while F_{i0} is a feed rate which is constant. After the integration, we obtain

$$\int_0^V \frac{dV}{F_{i0}} = \int_0^{X_{if}} \frac{dX_i}{-r_i}$$

$$\frac{V}{F_{i0}} = \frac{\tau}{C_{i0}} = \int_0^{X_{if}} \frac{dX_i}{-r_i} \tag{17}$$

$$\tau = \frac{V}{v_0} = \frac{VC_{i0}}{F_{i0}} = C_{i0} \int_0^{X_{if}} \frac{dX_i}{-r_i} \tag{18}$$

Where τ is time for complete conversion of a reactant particle to product and v_0 is volumetric flow rate (volume of fluid/time). With a given feed rate (F_{i0}), reactor size (V), and kinetic rate expression (r_i), a required conversion can be determined by Eq. (17). Thus, the concentration of each reactant i at outlet of reactor can be determined through a known conversion and the concentration of each product j at outlet of reactor will be determined by a stoichiometry of a reaction.

With the basic of species material balance by the plug flow model, the overall material balance schematic for the conventional steam methanol reforming (SMR) process and the sorption-enhanced steam methanol reforming (SE-SMR) process are briefly described in Fig 4-5.

CH$_3$OH, H$_2$O (mol/h) →

CH$_3$OH, H$_2$O, CO, CO$_2$, H$_2$ (mol/h)
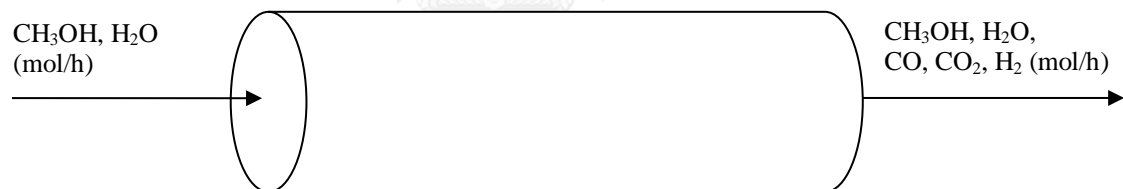
Fig. 4   Material balance for the conventional SMR process

Regenerated CaO (mol/h)
CH$_3$OH, H$_2$O (mol/h) →

Spent CaO (mol/h)
CH$_3$OH, H$_2$O, CO, CO$_2$, H$_2$ (mol/h)

Fig. 5   Material balance for the SE-SMR process

3.4.2 RStoic reactor model

RStoic or stoichiometric reactor is a reactor model provided in Aspen Plus software. RStoic models a reactor when reaction kinetic is unknown or unimportant and stoichiometry of reaction is known. RStoic calculates the product stream flow rate based on user-specified reaction stoichiometry and extent of reaction or conversion of a key component (Aspen Plus Version 8.2., 2014). Apart from the steam methanol reformers, other reactors were simulated based on RStoic reactor as they were not the main issue for study. To find out which reactor is based on RStoic reactor, see the categorization in CHAPTER IV.

3.4.3 Heat balance

For the modeling of an isothermal reactor, either external cooling or heating is considered to maintain reactor temperature. The reactor is modeled by specifying the reactor temperature, Aspen plus then automatically calculates the heat duty consumed or generated due to reactions taken place in the reactor. The heat balance is also solved by the iterative method. The heat balance for isothermal reactor in steady state condition is expressed in Eq. (19) as follows:

$$\dot{H}_{input} + \dot{Q}_{input} - \dot{H}_{output} - \dot{Q}_{output} = 0 \tag{19}$$

Where $\dot{H}_{input}$ is enthalpy or rate of energy added by mass flow into a reactor. $\dot{Q}_{input}$ is rate of flow of heat to a reactor from external heating. $\dot{H}_{output}$ is enthalpy or rate of energy leaving by mass flow out of a reactor. $\dot{Q}_{output}$ is rate of flow of heat leaving a reformer by external cooling.

3.5   Sequential quadratic programming

Sequential quadratic programming (SQP) is an iterative method used for the optimization in this work. Sequential quadratic programming is a default optimization procedure in Aspen Plus software, its rigorous module is attached in Aspen Plus for optimization. It is a technique for the solution of Nonlinear Programming (NLP) problems (Gockenbach, 2003). All equality and inequality constraints in NLP problems can be solved by the SQP method (Hoppe, 2006). The SQP method uses a quadratic model for the objective function and a linear model for the constraint (Gockenbach, 2003).

3.6   Heat integration and heat exchanger network

The heat integration has been used in many process industrial designs to minimize the cost of utilities required for the process. All guidelines and procedures below are summarized from the book of Chemical Process Design and Integration by Smith a,b (2005). The possible heat recovery from the hot streams to the cold streams is determined by the analysis of existing heat exchanger network and composite curves of hot and cold streams (Pinch Analysis). A new heat exchanger network design including the energy exchanged between hot and cold streams regarding the heat recovery analysis is later performed by the "tick-off" heuristic and the "grid diagram". Details for these methodologies are described in CHAPTER V, section 5.3.

CHAPTER IV

METHODOLOGY

The conventional steam methanol reforming (SMR) process and the sorption-enhanced steam methanol reforming (SE-SMR) process were theoretically studied using Aspen Plus simulator. The RPlug model based on the methanol reforming reactions, i.e., methanol steam reforming, methanol decomposition, water gas shift reaction, and carbonation (Eqs. (1)-(3) and Eq. (9)) was used to simulate the reformer. The kinetic models of the reactions (Eqs. (1)-(3)), developed by Peppley et al. (1999) using $Cu/ZnO/Al_2O_3$ catalyst were used, whereas the carbonation reaction (Eq. (9)) was based on the intrinsic rate of the $CaO\text{-}CO_2$ reaction developed by Sanchez et al. (2012). The $CaO\text{-}CO_2$ reaction was based on Arctic Dolomite (CaO-based sorbent) and its kinetic constant developed by Sun et al. (2008) was employed. Several basic assumptions for the simulations were made as depicted in Section 4.1.1-4.1.2. Details for simulation of the conventional steam reforming process and the sorption-enhanced steam reforming process are described in Section 4.1.3-4.1.4.

4.1 Basic assumptions and details for simulation of conventional and sorption-enhanced steam methanol reforming (SMR and SE-SMR)

4.1.1 Basic assumptions for simulation of conventional steam reforming

a) Process is under steady state and isothermal conditions.

b) Gases and solid catalyst are uniformly distributed within the reformer.

c) Conventional steam reformer is designed based on a one-dimensional fixed bed reactor model.

d) A pseudo-homogeneous reaction system is assumed.

4.1.2 Basic assumptions for simulation of sorption-enhanced steam reforming

a) Process is under steady state and isothermal conditions.

b) Gases, solid catalyst, and CaO sorbent are uniformly distributed within the reformer.

c) Sorption-enhanced steam reformer is designed based on a one-dimensional moving bed reactor model.

d) As CaO sorbent in a reactor behaves like a moving bed, the sorbent is designed to continuously circulate in the sorption-enhanced steam reformer with the same rate of fresh sorbent input and spent sorbent output. Hence, the sorbent bed inside a reactor is considered fresh at all time.

e) A pseudo-homogeneous reaction system is assumed and the specific surface area of the sorbent is assumed to be constant since fresh sorbent is assumed throughout the reforming operation.

4.1.3   Simulation of conventional steam methanol reforming (SMR)

The conventional steam methanol reforming (SMR) process was simulated using Aspen Plus based on "Peng Robinson" equation of state property model. The integrated system of the conventional steam reforming process included methanol steam reformer, water gas shift reactor, and preferential oxidation reactor. The process flow diagram of the conventional steam methanol reforming in this work is shown in Fig. 6.
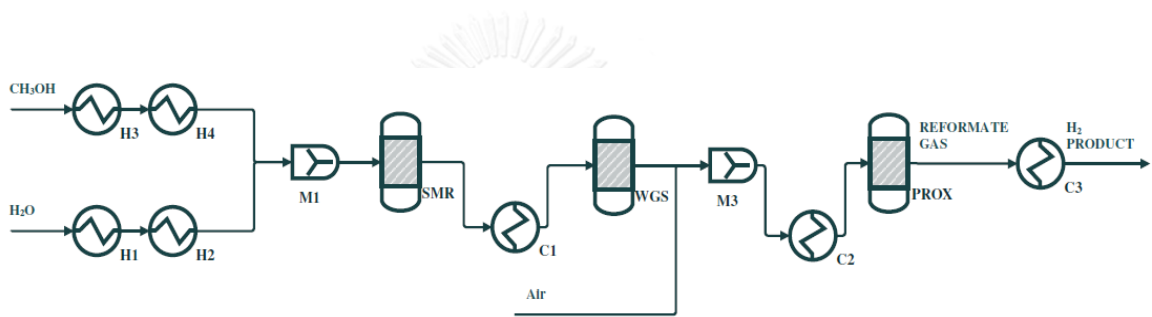
Fig. 6   Process flow diagram of conventional steam methanol reforming process used in this work

Water and liquid methanol were separately fed to vaporizers H1 and H3. Each of the vaporized reactant streams was then heated by heat exchangers H2 and H4 to steam methanol reformer (SMR) operating temperature. Methanol and steam would react in the reformer via multiple reaction paths resulting in a mixture of H_2, CO_2 and CO. Main reactions that took place in the reformer were methanol steam reforming, water gas shift reaction, and methanol decomposition. A fixed bed reactor containing solid catalyst was designed for the reformer based on a plug flow model. To complete a plug flow modeling, kinetic rate expressions of all reactions were required. In this study, the kinetic models with respect to $Cu/ZnO/Al_2O_3$ catalyst developed by

Peppley et al. (1999) were used to simulate the reformer. Rate of reactions used in the plug flow model were based on catalyst bed volume fixed in the reactor, bed volume and void fraction are presented in Table 5. Methanol feed rate was fixed at 2.5 mol/h, steam fed to the reformer was varied from 2.5 mol/h to 15 mol/h, S/C feed ratio was from 1 to 6. S/C feed ratio is defined in Eq. (20) and used throughout the study.

$$\text{S/C feed ratio} = \frac{\text{moles of steam fed to system}}{\text{moles of methanol fed to system}} \tag{20}$$

The reformer temperature would be optimized in the temperature range of 200-400 °C. The reformer effluent was cooled down to the operating condition of the water gas shift reactor at 220 °C by heat exchanger C1. By-product in the reformer effluent, CO, would react with the additional steam in the water gas shift reactor via water gas shift reaction in order to enhance the hydrogen production in the final reformate gas. Stoichiometric reactor based on 0.98 molar fractional conversion of CO was used to model the water gas shift reactor operating at 220 °C with H_2O/CO feed ratio higher than 3.5 (Choi & Stenger, 2003).

$$\text{H}_2\text{O/CO feed ratio} = \frac{\text{moles of steam fed to system}}{\text{moles of CO fed to system}} \tag{21}$$

These conditions were chosen from several conditions investigated by Choi and Stenger (2003) as these conditions can yield high CO conversion at low temperature. $Cu/ZnO/Al_2O_3$ catalyst was chosen for the water gas shift reactor. According to the limitation of thermodynamic equilibrium through the water gas shift reaction (Martinez et al., 2013), 100% conversion of CO cannot be attained resulting in high CO content in the water gas shift reactor effluent. Based on hydrogen product for the proton exchange membrane (PEM) fuel cell, the maximum value for CO impurity in

hydrogen product allowed in the PEM fuel cell is 10 ppm, otherwise catalyst poisoning of the platinum catalyst at PEM fuel cell anode will occur (Martinez et al., 2013). The final step to reduce such impurity was to eliminate them through the preferential oxidation reactor (PROX). The gas product stream from the water gas shift reactor and air was mixed and cooled down by heat exchanger C2 to 200 °C which is the optimal operating temperature of the preferential oxidation reactor based on Pt/Al$_2$O$_3$ catalyst as reported by Chang and Tatarchuk (2003). Stoichiometric reactor was once more used to model the preferential oxidation reactor. From the literature review (Chang & Tatarchuk, 2003), the maximum CO molar conversion was achieved at 100% via CO oxidation reaction at the temperature of 200 °C and O$_2$/CO feed ratio of 1. Small amount of hydrogen was converted to water owing to the hydrogen oxidation reaction; hydrogen conversion was about 0.04 % based on 55% oxygen selectivity for CO oxidation reaction.

$$\text{O}_2/\text{CO feed ratio} = \frac{\text{moles of O}_2 \text{ fed to system}}{\text{moles of CO fed to system}} \qquad (22)$$

$$\text{H}_2 \text{ conversion (\%)} = \frac{\text{moles of H}_2 \text{ fed to system - moles of H}_2 \text{ leaving system}}{\text{moles of H}_2 \text{ fed to system}} \times 100 \quad (23)$$

$$\text{O}_2 \text{ selectivity (\%)} = \frac{\text{O}_2 \text{ consumption by CO oxidation}}{\text{Total O}_2 \text{ consumption}} \times 100 \qquad (24)$$

Finally, the reformate gas temperature was reduced by heat exchanger C3 to the feeding temperature of the PEM fuel cell at 80 °C. Main process parameters used for simulating the conventional system are depicted in Table 5.

Table 5   Main process parameters for conventional steam methanol reforming

Process parameters	Methanol steam reformer	Water gas shift reactor	PROX reactor
Reactor model	RPLUG (based on kinetic models)	RSTOIC (based on 90% conversion of CO)	RSTOIC (based on 0.24% conversion of H_2 and 100% conversion of CO)
Operating temperature (°C)	200-400	220	200
S/C feed ratio	1-6	-	-
H_2O/CO feed ratio	-	> 3.5	-
O_2/CO feed ratio	-	-	1
Reactor length (cm)	19.6	-	-
Reactor diameter (cm)	2.5	-	-
Catalyst	$Cu/ZnO/Al_2O_3$	$Cu/ZnO/Al_2O_3$	Pt/Al_2O_3
Catalyst density (kg/m^3)	1300	1300	-
Void fraction	0.5	-	-
Reaction	- Methanol steam reforming - Methanol decomposition - Water gas shift reaction	- Water gas shift reaction	- CO oxidation - Hydrogen oxidation

4.1.4   Simulation of sorption-enhanced steam methanol reforming(SE-SMR)

The sorption-enhanced steam methanol reforming (SE-SMR) process was simulated using Aspen Plus based on "Peng Robinson" equation of state property model. Sorption-enhanced steam reforming process consisted of two major components: sorption-enhanced steam reformer and regeneration unit. The simulation of sorption-enhanced steam reformer was based on a plug flow model. Reactions occurred in both conventional and sorption-enhanced steam reformer were the same, except that there was carbonation of CaO-CO_2 taken place in the sorption-enhanced steam reformer. Reaction rates for methanol steam reforming, water gas shift reaction,

and methanol decomposition were based on the catalyst bed volume, whereas the carbonation reaction was based on the CaO-based sorbent volume in the reformer. Bed volumes of the catalyst and sorbent used in the sorption-enhanced steam reformer and void fraction are presented in Table 6. The process flow diagram of the sorption-enhanced steam methanol reforming in this work is shown in Fig. 7.

Water and liquid methanol were vaporized by heat exchangers H1 and H3, similar to the conventional process. Then both of gas streams were heated to the operating temperature of the sorption-enhanced steam reformer by heat exchangers H2 and H4. Methanol feed rate was fixed at 2.5 mol/h. Steam fed to the reformer was varied from 2.5 mol/h to 15 mol/h, or from 1 to 6 in terms of S/C feed ratio. The sorption-enhanced steam reformer temperature would be optimized in the temperature range of 200-400 °C. As reported by Martinez et al. (2013), the final reformate gas can achieve high hydrogen purity and low CO concentration (< 10 ppm) by a single step of sorption-enhanced steam reformer, which means further treatment for reformate gas is not required. Finally, the reformate gas temperature was reduced by heat exchanger C1 to the feeding temperature of the PEM fuel cell at 80 °C.
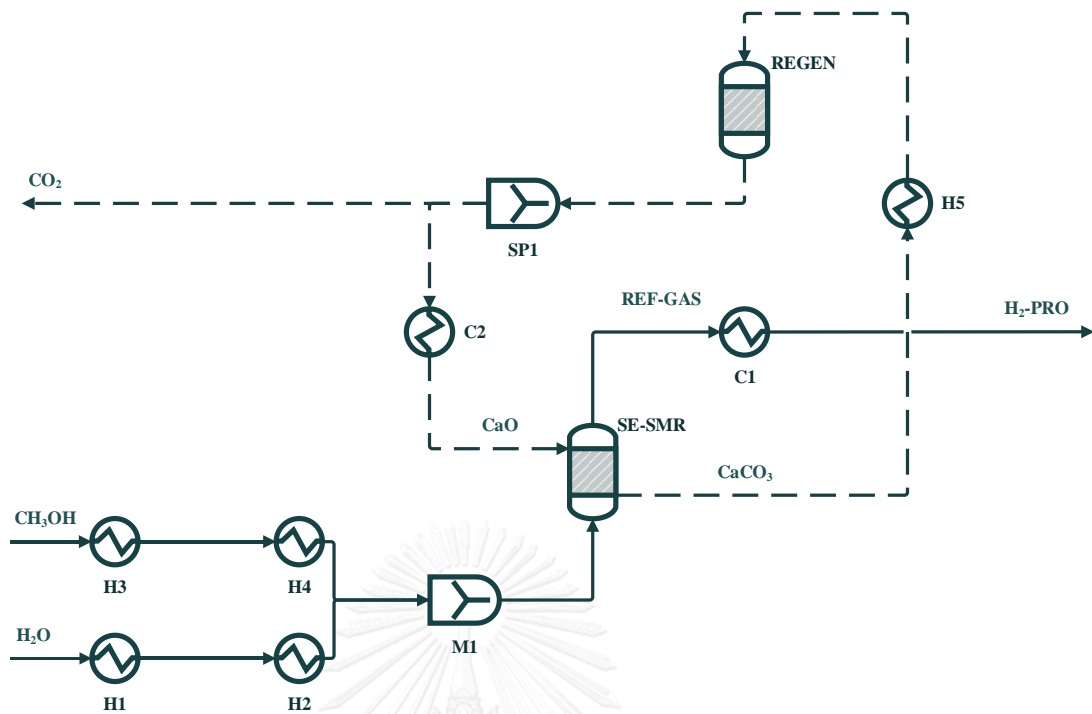
Fig. 7   Process flow diagram of sorption-enhanced steam methanol

reforming process used in this work

Regeneration system was also employed in this study to investigate heat consumption rate for overall process. The regenerator (REGEN) was modeled by stoichiometric reactor assuming to base on $CaCO_3$ molar fractional conversion of 1.0. Fresh CaO sorbent was assumed to be continuously fed to the reformer while the spent sorbent was removed to the regeneration unit. Both input and output rate of CaO sorbent regarding the reformer was assumed to be equivalent to the regeneration rate of $CaCO_3$.

According to this study, $CaCO_3$ was heated to the regeneration temperature of 850 °C by heat exchanger H5 and turned into fresh CaO with CO_2 desorbed via calcination reaction in the regenerator. Gas-solid mixture of $CaO\text{-}CO_2$ leaving the

regenerator would be separated from each other via a cyclone which was presented by SP1. Then fresh CaO was cooled down to the reforming temperature by heat exchanger C2 and was, again, fed to the reformer.

An amount of CaO volume inside the sorption-enhanced steam methanol reformer was varied by a sorbent-to-catalyst volume ratio (λ) between 0.15 and 0.90 to study the performance of the sorption-enhanced steam reforming process. The catalyst volume used in the sorption-enhanced steam reformer was fixed base on the volume used in the study of the conventional steam methanol reformer. Hence, the reactor volume and reactor length of the sorption-enhanced steam reformer were higher than that obtained from the conventional steam reformer. Main process parameters for simulating the sorption-enhanced steam reforming system are depicted in Table 6.

Table 6　Main process parameters for sorption-enhanced steam methanol reforming

Process parameters	Sorption-enhanced methanol steam reformer	Regenerator
Reactor model	RPLUG (based on kinetic models)	RSTOIC (based on 100% conversion of $CaCO_3$)
Operating temperature (°C)	200-400	850
S/C feed ratio	1-6	-
Reactor length (cm)	22.5-37.2	-
Reactor diameter (cm)	2.5	-
Catalyst	Cu/ZnO/Al2O3	-
Catalyst density (kg/m3)	1300	-
Sorbent	Arctic dolomite	-
Sorbent-to-catalyst volume ratio (λ)	0.15-0.90	-
Void fraction	0.5	

Table 6   Main process parameters for sorption-enhanced steam methanol reforming (continued)

Process parameters	Sorption-enhanced methanol steam reformer	Regenerator
Reaction	- Methanol steam reforming - Methanol decomposition - Water gas shift reaction - Carbonation	- Calcination

จุฬาลงกรณ์มหาวิทยาลัย
CHULALONGKORN UNIVERSITY

4.2   Scope of the study

The mentioned basic assumptions and simulation steps of both the conventional steam reforming process and the sorption-enhanced steam reforming process were applied to the study. The outline of the thesis scope is summarized in Fig. 8 as seen below. Details of the study are depicted in Section 4.2.1-4.2.4.
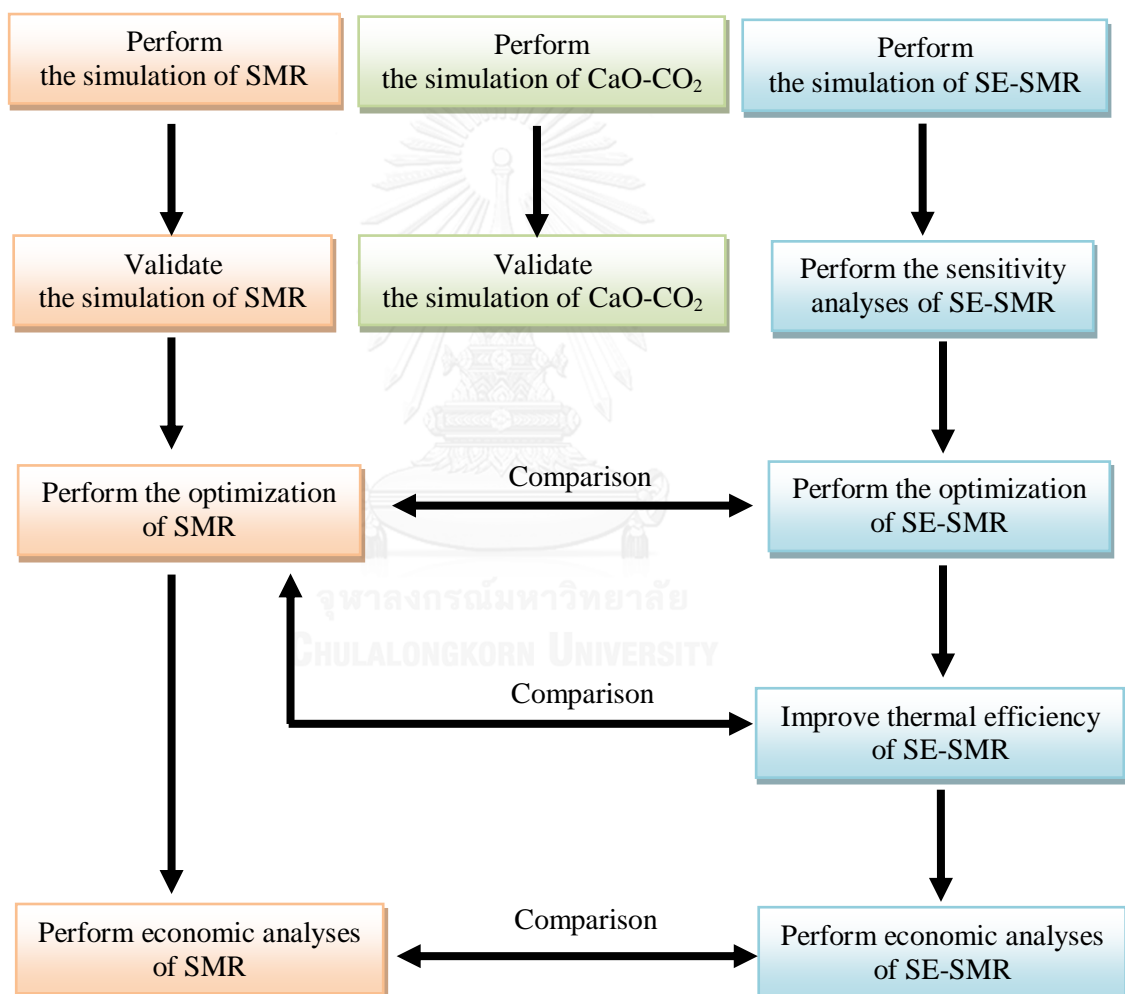
Fig. 8   Outline of the thesis scope

There are several parameters used in the evaluation of the system performance of the sorption-enhanced steam methanol reforming process, e.g., H_2 yield, CO concentration in final product, product concentration. To avoid confusion in the definition of these parameters, the notations used for evaluating performance are presented as follow:

$$H_2 \text{ concentration (mol \% dry basis)} = \frac{\text{moles of } H_2 \text{ in gas product}}{\text{moles of } H_2, CO, CO_2 \text{ in gas product}} \times 100 \quad (25)$$

$$CO \text{ concentration (ppm dry basis)} = \frac{\text{moles of CO in gas product}}{\text{moles of } H_2, CO, CO_2 \text{ in gas product}} \times 10^6 \quad (26)$$

$$\text{Product gas concentration, } H_2 \text{ (mol \% dry basis)}$$
$$= \frac{\text{moles of } H_2 \text{ in gas product}}{\text{moles of total gas product excluding } H_2O} \times 100 \quad (27)$$

$$\text{Product gas concentration, } CO_2 \text{ (mol \% dry basis)}$$
$$= \frac{\text{moles of } CO_2 \text{ in gas product}}{\text{moles of total gas product excluding } H_2O} \times 100 \quad (28)$$

$$\text{Product gas concentration, } CO \text{ (mol \% dry basis)}$$
$$= \frac{\text{moles of CO in gas product}}{\text{moles of total gas product excluding } H_2O} \times 100 \quad (29)$$

$$\text{Product gas concentration, } CH_3OH \text{ (mol \% dry basis)}$$
$$= \frac{\text{moles of } CH_3OH \text{ in gas product}}{\text{moles of total gas product excluding } H_2O} \times 100 \quad (30)$$

$$\text{Methanol conversion (\%)}$$
$$= \frac{\text{moles of } CH_3OH \text{ fed to system - moles of } CH_3OH \text{ leaving system}}{\text{moles of } CH_3OH \text{ fed to system}} \times 100 \quad (31)$$

$$H_2 \text{ yield} = \frac{\text{moles of } H_2 \text{ produced}}{\text{moles of } CH_3OH \text{ fed to the system}} \quad (32)$$

4.2.1 Sensitivity analyses of sorption-enhanced steam methanol reforming (SE-SMR)

Sensitivity analyses of key operating parameters of the sorption-enhanced steam reformer of methanol were performed in the temperature range of 200-400 °C. S/C feed ratio was varied from 1 to 6. Another one important parameter for the sensitivity analyses of the sorption-enhanced steam reforming was a sorbent-to-catalyst volume ratio (λ) which was varied from 0.15 to 0.90. Results from the sensitivity analyses were used to study the performance of the sorption enhanced steam methanol reforming at different operating conditions. Moreover, it was useful for the analyses in other sections.

4.2.2 Optimization of sorption-enhanced and conventional steam methanol reforming (SE-SMR and SMR)

Optimization of the sorption-enhanced steam methanol reforming was performed with the aim to determine optimal design parameters for maximizing the H_2 yield. To make a comparison with the optimal design parameters obtained from the conventional SMR, the optimization was applied to the conventional SMR based on the maximum hydrogen produced by the SE-SMR. The optimization problem was formulated with a constraint on the CO concentration in the final product below 10 ppm on dry basis and solved by the sequential quadratic programming (SQP) module in Aspen Plus. This produced hydrogen can be used in the fuel cell without the poisoning of anodic catalyst (Martinez et al., 2013). The optimization was done by a rigorous module of SQP attached in Aspen Plus software. Objective function, manipulated variable and its range for optimization, and constraint must be entered into the software input to begin the optimization. Details are presented as follow.

4.2.2.1 Optimization of sorption-enhanced steam methanol reforming (SE-SMR)

Regarding the optimization of the SE-SMR process, two cases with different objective functions were investigated to achieve the optimal operating conditions as presented below.

SE-SMR Case I: This case provided the optimization of the SE-SMR process with the maximization of H_2 yield. The constraint of this optimization problem was that the CO concentration must be below 10 ppm on dry basis. Results from the optimization showed that maximum hydrogen produced was 7.5 mol/h based on methanol feed of 2.5 mol/h.

SE-SMR Case II: This case provided the optimization of the SE-SMR process with the minimization of heat duty required by the steam reforming. This optimization problem had the same CO concentration constraint, below 10 ppm on dry basis. The objective function with maximum H_2 yield gave the high steam feed flow rate resulting in high heat duty required for the steam reforming. Thus, another case study for optimization with the minimization of heat duty required by the steam reforming was performed to find out another solution of optimal operating conditions. Results from the optimization showed that maximum hydrogen produced was 7.5 mol/h based on methanol feed of 2.5 mol/h. The objective functions, manipulated variables and constraints are summarized in Table 7.

Table 7   Optimization analysis tools of sorption-enhanced steam methanol reforming (SE-SMR)

Optimization tools	SE-SMR Case I	SE-SMR Case II
Objective function	Maximize: H_2 yield	Minimize: Reforming heat duty required*
Manipulated variable	S/C feed ratio: 1-6 Reforming temperature: 200-350 °C	S/C feed ratio: 1-6 Reforming temperature: 200-350 °C
Constraint	CO content: $\leq$ 10 ppm	CO content: $\leq$ 10 ppm

* Reforming heat duty required included heat required by heat exchangers H1, H2, H3, H4 and heat released by reactor SE-SMR, referring to Fig. 7.

4.2.2.2 Optimization of conventional steam methanol reforming(SMR)

To perform a comparison between the SE-SMR and conventional SMR processes, the optimization of the conventional SMR process in the reformer section was conducted to obtain the optimal operating conditions. The optimization of the conventional SMR process was performed in two cases with different objective functions as presented below.

SMR Case I: This case provided the optimization on the conventional steam reformer with the maximization of H_2 yield. As the CO concentration leaving the conventional reformer cannot be less than 10 ppm on dry basis, the constraint of CO concentration was not applied in this case of optimization. Hence, the constraint for this case of optimization would be an amount of hydrogen product at 7.3 mol/h. At this constraint, the final hydrogen product could achieve 7.5 mol/h at the outlet of PROX reactor which is the same amount of hydrogen product obtained by the SE-SMR process based on methanol feed of 2.5 mol/h. However, the CO concentration in the final product of the conventional process was limited to less than 10 ppm on dry basis by PROX reactor.

SMR Case II: This case provided the optimization of the SMR process with the minimization of heat duty required by the steam reforming. The constraint for this case of optimization was an amount of hydrogen produced at 7.3 mol/h as same as the optimization for the SMR Case I. The objective functions, manipulated variables and constraints are summarized in Table 8.

Table 8   Optimization analysis tools of conventional steam methanol reforming (SMR)

Optimization tools	SMR Case I	SMR Case II
Objective function	Maximize: H_2 yield	Minimize: Reforming heat duty required*
Manipulated variable	S/C feed ratio: 1-6 Reforming temperature: 200-350 °C	S/C feed ratio: 1-6 Reforming temperature: 200-350 °C
Constraint	H_2 product: 7.3 mol/h	H_2 product: 7.3 mol/h

* Reforming heat duty required included heat required by heat exchangers H1, H2, H3, H4 and heat required by reactor SMR, referring to Fig. 6.

4.2.3 Heat integration of sorption-enhanced steam methanol reforming (SE-SMR) process

Heat integration was performed in the sorption-enhanced steam methanol reforming (SE-SMR) process under the optimal condition in order to reduce energy consumed by the process. Heat exchanger network design by the "pinch analysis" was applied to the process, heat recovery was determined and hot utility required was reduced. The composite curves of hot and cold streams played an important role to determine the possible heat recovery within the process. Later, the heat exchanger network of the SE-SMR process was designed by the "tick-off" heuristic and the "grid diagram". Finally, the thermal efficiency of the SE-SMR process was evaluated and

compared with the conventional SMR process. Details of the heat integration are illustrated in CHAPTER V.

4.2.4 Economic analyses of sorption-enhanced steam methanol reforming (SE-SMR) process

A simple profit estimation of the sorption-enhanced steam methanol reforming (SE-SMR) process was calculated under the optimal condition. The profit was based on selling price of hydrogen and cost of production; the cost of production was the sum of fixed cost and operating cost. As a small-scale reforming at a refueling station is attractive in near-term to mid-term for supplying hydrogen to vehicles (Ogden, 2001), the selling price of hydrogen would be based on hydrogen produced from the reforming process at the on-site hydrogen refueling station which is sold as a fuel supply for the fuel cell vehicles (Hill & Penev, 2014). However, the cost of compression unit for hydrogen storage and distribution was added to the profit estimation to complete the economic analysis for overall processing of hydrogen production and distribution. Results were compared with the conventional SMR process.

4.3   Model validation of conventional steam methanol reforming (SMR) and carbonation reaction

An ideal plug flow reactor modeled by Aspen Plus was validated with published data to confirm its reliability. The validation was separated into two parts, validation for the conventional steam methanol reforming (SMR) and validation for the CaO-CO$_2$ reaction in a plug flow reactor.

4.3.1   Validation of conventional steam methanol reforming (SMR) in a plug flow reactor

The kinetic models developed by Peppley et al. (1999), as indicated in Eqs. (4)-(6), are well-known and are used in many literatures related to the methanol steam reforming using Cu/ZnO/Al$_2$O$_3$ catalyst (Ghasemzadeh et al., 2013; Lotric & Hocevar, 2012; Purnama, 2003 ; S. T. Sa, 2011; Telotte et al., 2008; Vadlamudi & Palanki, 2011). To validate the characteristic and performance of the plug flow reactor for the conventional steam methanol reforming, methanol conversion and CO molar fraction at the outlet of the reformer as the simulation output using kinetic models of Peppley et al. (1999) were compared to available experimental results reported by S.T. Sa (2011). Based on methanol feed rate of 1 mol/s, catalyst loading at 15 kg, S/C feed ratio of 1.5, and pressure at 1 bar, methanol conversion (%), defined by Eq. (33), and CO molar fraction, defined by Eq. (34) are summarized against the reforming temperature and shown in Tables 9-10.

Methanol conversion:

$$X_{CH_3OH} = \frac{F_{CO}^{out} + F_{CO_2}^{out}}{F_{CH_3OH}^{in}}$$

(33)

where F_{CO}^{out} is the molar flow rate of carbon monoxide leaving the reactor, $F_{CO_2}^{out}$ is the molar flow rate of carbon dioxide leaving the reactor, and $F_{CH_3OH}^{in}$ is the molar flow rate of methanol fed to the reactor.

CO molar fraction:

$$y_{CO} = \frac{F_{CO}^{out}}{F_{Total}^{out}} \tag{34}$$

where F_{Total}^{out} is the molar flow rate of overall product leaving the reactor.

Table 9   Result of methanol conversion (%) against reforming temperature (200-300 °C) obtained from simulation and experiment (S. T. Sa, 2011)

Temperature (°C)	Methanol conversion (%) from simulation	Methanol conversion (%) from experiment (S. T. Sa, 2010)	Error (%)
200	24.18	24.00	0.73
220	47.71	47.00	1.52
230	61.50	58.00	6.04
240	74.80	72.00	3.89
250	86.02	80.00	7.52
265	96.54	93.00	3.81
280	99.73	96.00	3.89
300	100.00	98.00	2.04

Table 10   Result of CO molar fraction against reforming temperature (200-300 °C) obtained from simulation and experiment (S. T. Sa, 2011)

Temperature (°C)	CO molar fraction from simulation	CO molar fraction from experiment (S.T. Sa, 2010)	Error (%)
200	2.28×10^{-4}	0	N/A*
220	9.97×10^{-4}	9.38×10^{-4}	6.40
230	2.00×10^{-3}	1.88×10^{-3}	6.91
240	3.88×10^{-3}	3.75×10^{-3}	3.35
250	7.06×10^{-3}	6.70×10^{-3}	5.35
265	1.46×10^{-2}	1.38×10^{-2}	6.51
280	2.37×10^{-2}	2.30×10^{-2}	2.99
300	3.44×10^{-2}	2.90×10^{-2}	18.54

* N/A is "Not Applicable".

As shown in Table. 9, methanol conversion from the simulation and the experiment increased with increasing reforming temperature. Methanol conversions from the simulation comparing with the experiment along the reforming temperature behaved in the same fashion, though with error of 0.73-7.52%. The model fitting for CO molar fraction at the outlet of the reactor was also performed to confirm the accuracy of the plug flow model using in Aspen Plus simulator. Table 10 showed that CO molar fractions from the simulation with respect to the experiment had the same trend with percentage error of 2.99-6.91%. However, the percentage error of 18.54% was excluded from the validation since the error extremely deviated from others. Percentage error was determined as illustrated in Eq. (35).

$$\text{Error (\%)} = \frac{\text{Simulaiton data} - \text{Experiment data}}{\text{Experiment data}} \times 100 \tag{35}$$

As the plug flow model was assumed based on a pseudo-homogeneous system, the negligence of mass-transfer limitations inside the catalysts caused

overestimation of methanol conversion and CO molar fraction. Hence, methanol conversion and CO molar fraction from the simulation results were higher than that obtained from the experiment.

4.3.2 Validation of carbonation reaction in a plug flow reactor

Based on the reaction rate of carbonation or CO_2 adsorption by CaO, the intrinsic rate constant and the activation energy were found to vary with regards to CaO-based sorbent. To validate the characteristic and performance of the plug flow reactor for the carbonation reaction, CaO conversion resulting from the simulation was compared with the available experimental results by Sedghkerdar et al. (2014). The validation was based on the reaction rate of the carbonation by Cadomin limestone, CaO-based sorbent . The comparison was illustrated in Table. 11. As indicated in the literature, the CaO conversion is expressed in Eq. (36) as seen below (Sedghkerdar et al., 2014).

CaO conversion:

$$CaO \, conversion = \frac{m(t) - m(0)}{44} / \frac{m(0) \, x \, Purity}{56} \tag{36}$$

where $m(0)$ is the amount of CaO-based sorbent at time zero (g), $m(t)$ is the amount of CaO-based sorbent at time t (g) and Purity is the CaO wt.% in the Cadomin limestone (46.99%). It is noted that the molecular weight of CO_2 is 44 g/mol and the molecular weight of CaO is 56 g/mol.

Table 11   Result of CaO conversion against carbonation temperature (500-675 °C) obtained from simulation and experiment (Sedghkerdar et al., 2014)

Temperature (°C)	CaO conversion from simulation	CaO conversion from experiment (Sedghkerdar et al., 2014)	Error (%)
500	0.78	0.76	2.04
550	0.94	0.88	7.29
600	1.00	0.93	7.53
675	1.00	0.95	5.26

The comparison between CaO conversion from the simulation and the experiment showed a good agreement. Percentage error (Eq. (35)) of CaO conversion from the simulation comparing to the experiment was in a range of 2.04-7.53%. An overestimation of CaO conversion by the simulation resulted by neglecting the diffusion rate of the carbonation reaction. Carbonation reaction can theoretically occur under two controlling reaction regimes, chemical reaction control regime and diffusion control regime (D.K. Lee et al, 2004 cited in Rashidi, 2012). The first regime of the reaction occurred rapidly by heterogeneous surface chemical reaction kinetics. When $CaCO_3$ layer, product of carbonation reaction, forms at the outer surface of CaO, the reaction rate will decrease due to the diffusion limitations of reactants through such layers . As the carbonation reaction in the simulation was based on only chemical reaction regime, the overestimation of CaO conversion was occurred with respect to the experiment.

CHAPTER V

RESULT AND DISCUSSIONS

5.1 Sensitivity analyses of sorption-enhanced steam methanol reforming (SE-SMR)

5.1.1 Effect of sorbent to catalyst volume ratio (λ) in reactor

The effect of sorbent-to-catalyst volume ratio (λ) in the reactor was studied in the temperature range of 200-400 °C, S/C feed ratio of 2, and methanol feed flow rate of 2.5 mol/h. H_2 concentration in the final product of the SE-SMR in mol% dry basis as a function of sorbent-to-catalyst volume ratio (λ) and reforming temperature is shown in Fig. 9. At the same reforming temperature, results showed that H_2 concentration increased when λ was increased. The increasing H_2 concentration results from the removal of CO_2 by CaO sorbent. The removal of CO_2 causes the equilibrium of methanol steam reforming reaction and water gas shift reaction to shift to the side that promotes H_2 production according to the Le Chatelier's principle (Peng, 2003). Le Chatelier's principle is the principle used for explaining a disturbance in chemical equilibrium reaction, when one of the products in the equilibrium reaction is removed from the reaction zone, the conversion of reactants to products and the rate of forward reaction can be increased (Peng, 2003). At constant sorbent-to-catalyst volume ratio, H_2 concentration increased with increasing reforming temperature. Moreover, results showed that the reaction at lower sorbent-to-catalyst volume ratio required higher reforming temperature compared with the

reaction at higher sorbent-to-catalyst volume ratio to achieve the same H_2 concentration.

From the investigation, it can be concluded that the sorbent-to-catalyst volume ratio affects H_2 concentration and reforming temperature. In order to achieve H_2 product specification with appropriate reforming temperature while expending minimal amount of sorbent, optimization of the sorbent was performed.
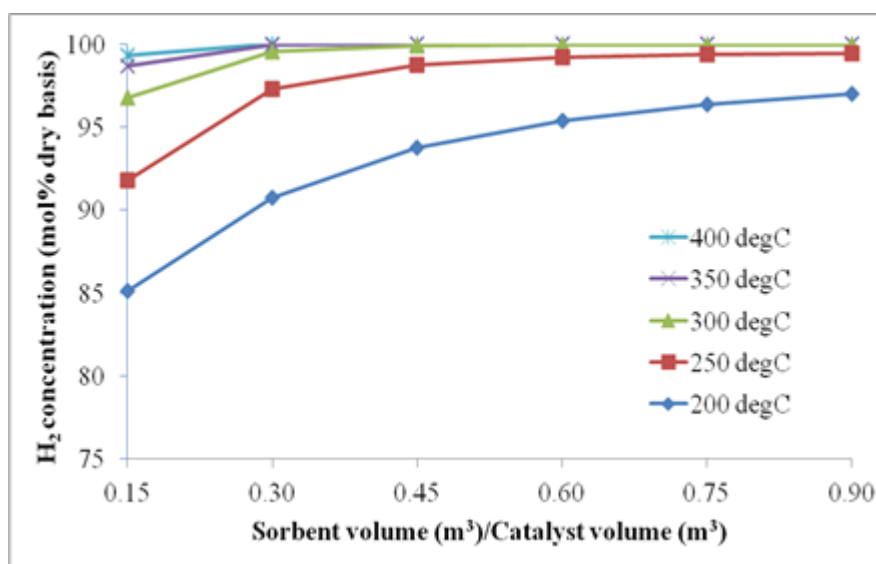
Fig. 9 H_2 concentration (mol% dry basis) as a function of sorbent-to-catalyst volume ratio (λ) (Temperature = 200-400 °C, S/C = 2, CH_3OH = 2.5 mol/h)

Figs. 10-11 show CO concentration in the final product of the SE-SMR in ppm dry basis as a function of sorbent-to-catalyst volume ratio (λ) and reforming temperature. Results were shown in the temperature range of 330-400 °C to highlight the low CO concentration at high temperature. CO concentration at low temperature range of 200-330 °C was not considered in the study since the reforming in this temperature range provided very high CO concentration which was much greater than

the CO concentration limit at 10 ppm. The study illustrated that CO concentration in the final product exceeded 10 ppm for λ of 0.15-0.30 over the entire range of temperature (330-400 °C) and S/C feed ratio (1-6). The CO concentration at 10 ppm and lower could be achieved with λ of 0.45 and higher as presented in Fig. 11. Results showed that the reformer with low value of λ must be operated at sufficiently high temperature to obtain high purity hydrogen. Based on λ of 0.45, high H_2 concentration and low CO concentration at 10 ppm could be accomplished in the higher temperature range of 380-400 °C. Operating in high temperature range will limit the efficiency of the $Cu/ZnO/Al_2O_3$ catalyst which is degradable at the temperature higher than 350 °C (Choi & Stenger, 2005). However, higher steam feed rate could reduce the reforming temperature based on the same product specification as shown in the APPENDIX A. But it might lead to high energy required for vaporizing the water. Therefore, higher sorbent-to-catalyst volume ratio of 0.60 would be used in the following study to obtain the mild operating conditions for the catalyst at below 350 °C with high purity of hydrogen. Higher sorbent-to-catalyst volume ratio was not included in this study since excess sorbent consumes extra energy so as to heat itself up to the reaction temperature without gaining any advantage.
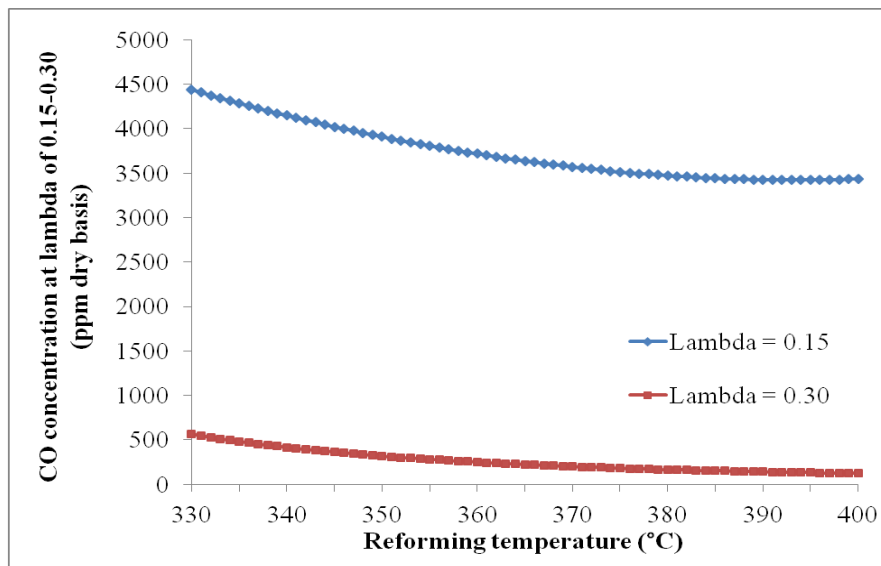
Fig. 10   CO concentration (ppm dry basis) as a function of λ and temperature

(Temperature =330-400 °C, S/C = 2, CH_3OH = 2.5 mol/h, λ = 0.15-0.30)
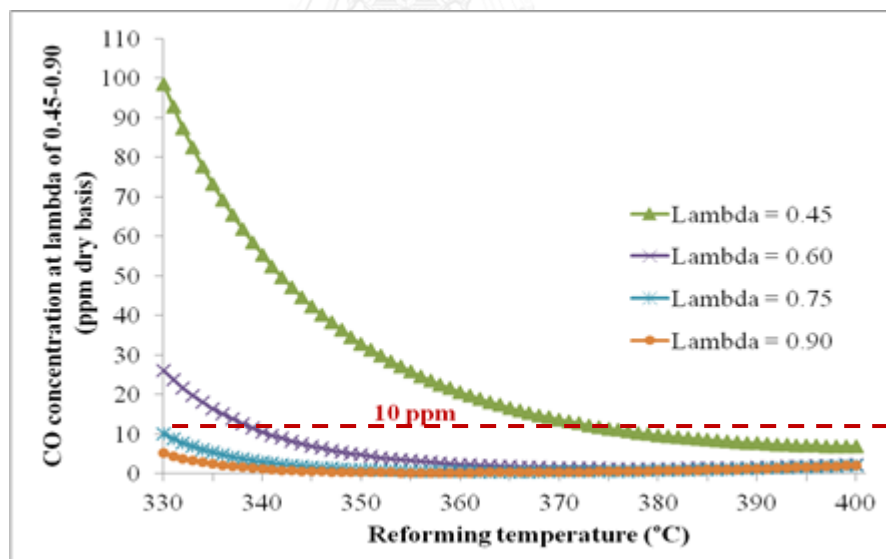
Fig. 11   CO concentration (ppm dry basis) as a function of λ and temperature

(Temperature =330-400 °C, S/C = 2, CH_3OH = 2.5 mol/h, λ = 0.45-0.90)

5.1.2 Effect of steam feed inlet to product distribution

Fig. 12 shows the concentration of simulated gas product by mol% on dry basis as a function of S/C feed ratio of 1-6. The concentration profiles were plotted at the temperature of 300 °C, λ of 0.60, and methanol feed rate of 2.5 mol/h. The simulation showed that by increasing S/C feed ratio from 1 to 2.75, the reaction produced higher amount of H_2 with reduced amount of CO_2 and CO. By adding more steam to the system, it reacts with the remaining CO and CH_3OH via water gas shift reaction and methanol steam reforming, respectively. This leads to higher H_2 and lower CO concentration, whereas CO_2 concentration decreased continuously by CaO-CO_2 reaction. Since the CaO conversion depends on partial pressure of CO_2 as reported by Sedghkerdar et al. (2014), having more CO_2 generated by water gas shift reaction and methanol steam reforming ultimately leads to better conversion of CaO and CO_2. In this range of S/C feed ratio, H_2 concentration increased from 97.02% and reach its peak at 99.93%. However, the concentration profiles were different in the range of S/C feed ratio of 2.75-6. The H_2 concentration decreased slightly while CO_2 concentration significantly increased as S/C feed ratio was increased. Having more fed into the reactor volume lowers resident time resulting in reduced conversion of CO_2 and less H_2 concentration. Moreover, for the H_2 concentration profile, higher CO_2 concentration adversely induces methanol steam reforming reaction to reverse based on the kinetic rate expressed in Eq. (5).
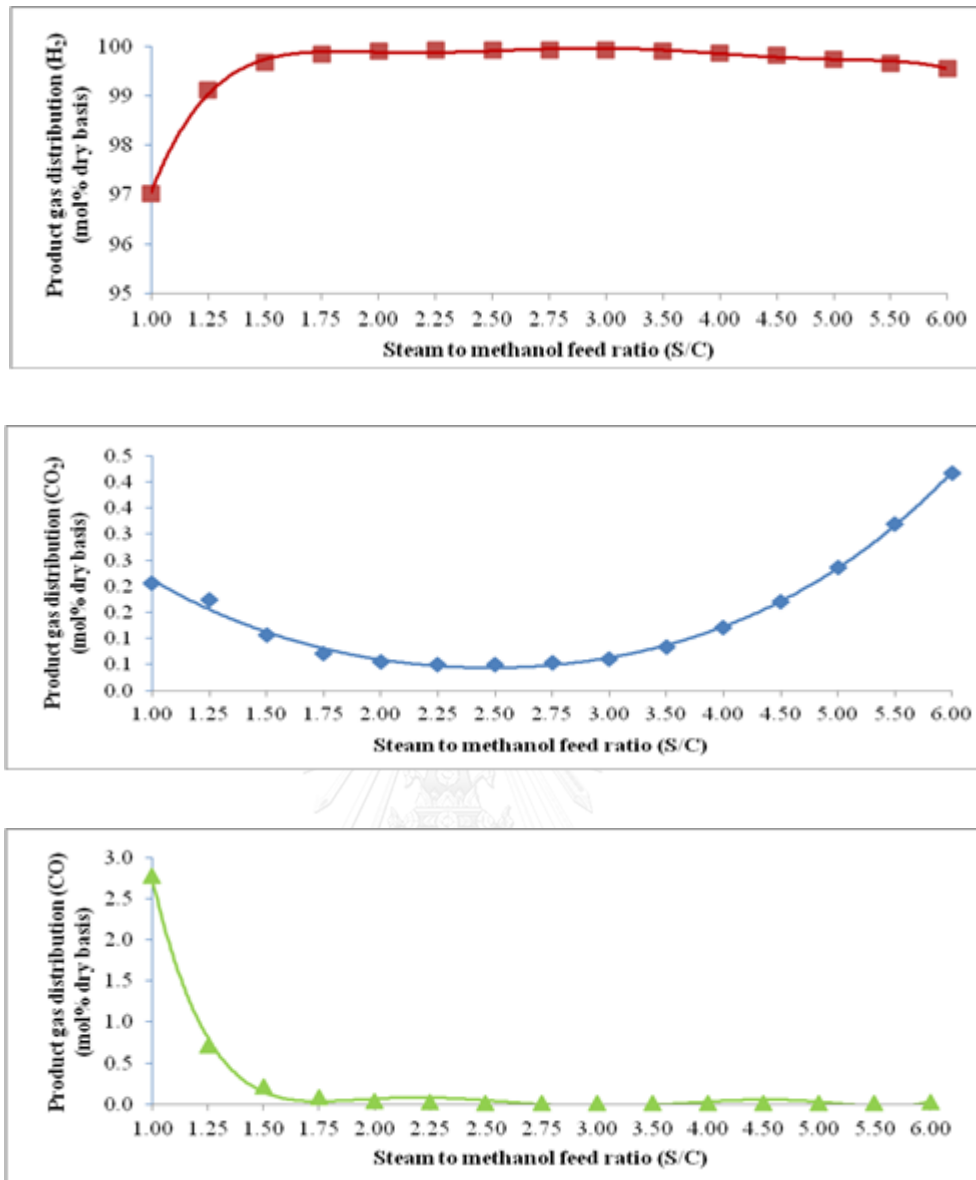
Fig. 12   Product gas concentration (mol% dry basis) as a function of S/C feed ratio

(Temperature = 300 °C, S/C = 1-6, CH_3OH = 2.5 mol/h, λ = 0.60)

5.1.3   Effect of reforming temperature to product distribution

Fig. 13 shows the concentration of simulated product gas on mol% dry basis as a function of reforming temperature of 200-400 °C. The concentration profiles were plotted at the S/C feed ratio of 2.75, λ of 0.60, and methanol feed flow rate of

2.5 mol/h. The plot showed that by increasing the reforming temperature, the reaction produced higher amount of H_2 owing to the condition that favors of methanol decomposition reaction and methanol steam reforming reaction. Results are in good agreement with the study of Katiyar et al. (2013); by performing the estimation of feasibility of reforming reactions via Gibbs free energy change concept, results showed that the change in Gibbs free energy of methanol decomposition and methanol steam reforming decreased with increasing reforming temperature.
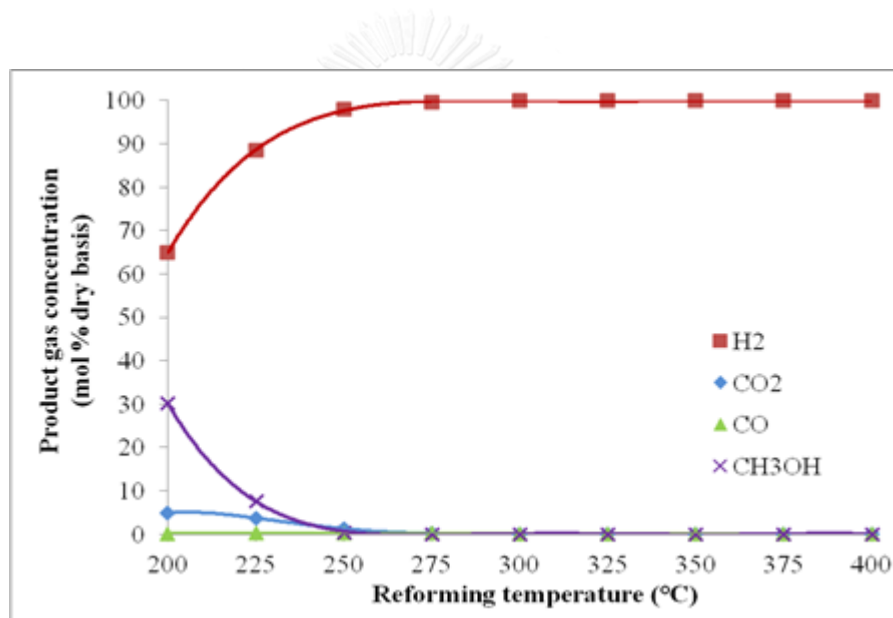
Fig. 13   Product gas concentration (mol% dry basis) as a function of reforming temperature (Temperature = 200-400 °C, S/C = 2.75, CH_3OH = 2.5 mol/h, λ = 0.60)

5.1.4 Effect of reforming temperature and S/C feed ratio to methanol conversion

Fig. 14 shows the plot of methanol conversion as a function of reforming temperature and S/C feed ratio. The simulations were performed in the temperature range of 200-400 °C and S/C feed ratio of 1-6. The plot showed that methanol

conversion increased with increasing reforming temperature. By increasing S/C feed ratio, methanol conversion decreased due to the reverse reaction of methanol steam reforming induced by high CO_2 as mentioned in Section 5.1.2. The conversion of methanol was 100% when the temperature increased to 250-270 °C.

Fig. 14   Methanol conversion (mol%) as a function of reforming temperature and

S/C feed ratio (Temperature = 200-400 °C, S/C = 1-6, CH_3OH = 2.5 mol/h, λ = 0.60)

5.1.5   Effect of reforming temperature and S/C feed ratio to H_2 yield and CO concentration

Fig. 15 shows the effect of reforming temperature and S/C feed ratio to H_2 yield. The simulation was performed in the temperature range of 200-400 °C and S/C feed ratio of 1-6. As seen in Fig. 15, maximum H_2 yield was achieved at 3 moles H_2 per mole CH_3OH. At the same reforming temperature, lower than 250 °C, the increase in S/C feed ratio led to lower H_2 yield. By having more steam fed into the reactor, the faster the reaction of methanol steam reforming and water gas shift will take place.

However, having more fed into the same reactor volume lowers resident time resulting in reduced conversion and less H_2 yield. At specific S/C feed ratio, it was obvious that H_2 yield increased along with temperature rose; since methanol decomposition and methanol reforming reactions are endothermic reaction, the reaction rate improves with the increase in temperature as mentioned in Section 5.1.3.

Fig. 15 H_2 yield as a function of reforming temperature and S/C feed ratio
(Temperature = 200-400 °C, S/C = 1-6, CH_3OH = 2.5 mol/h, λ = 0.60)

Fig. 16 shows the relation between reforming temperature and CO concentration at various S/C feed ratios. In the region lower than 250-280 °C, CO concentration increased along with temperature, because the temperature change within 200-400°C has insignificant effect on carbonation rate of reaction so the increase in temperature only favors methanol decomposition and methanol steam reforming. However, water gas shift reaction is used to explain the reduction in CO at low temperature since the reaction is thermodynamically preferable as reported by

Katiyar et al. (2013). In contrast to lower temperature, in the temperature range higher than 250-280 °C, CO concentration behaved inversely. The reason why CO concentration decreased while the temperature was increasing can be explained by the following steps:

- Once the temperature is increased, at some certain point, the sorption-enhanced steam methanol reforming (SE-SMR) exhausts methanol feed as studied in Section 5.1.4; methanol was completely converted at the temperature around 250-270 °C. By stepping up the temperature more, methanol steam reforming and water gas shift reaction can occur rapidly and introduce CO_2 earlier in the reactor instead of some being generated in the later section of reactor. The reason for this phenomenon is that a reaction at high temperature can deliver more activation energy to the particles and bring about more collision between particles. Hence, a rate of reaction increases with increasing temperature. The influence of temperature to a rate of reaction is explained by Arrhenius Equation and Collision Theory.

- For low temperature, reaction rates of methanol steam reforming and water gas shift occur slowly, so the produced CO_2 has less time to react with CaO. However, at elevated temperature, methanol steam reforming and water gas shift reaction occur rapidly at the early section of reactor which gives CO_2 more time to be adsorbed. However, it has been reported that the suppression in adsorption of CO_2 may be occurred by shortening the contact time (Li et al., 2012).

- Having more CO_2 adsorbed causes water gas shift reaction to shift to the higher H_2 production and consuming more CO resulting in low CO concentration according to the Le Chatelier's principle.

As for the effect from S/C feed ratio, feeding in more steam improves water gas shift reaction causing CO to diminish at constant temperature as explained by kinetic rate expression in Eq. (6).

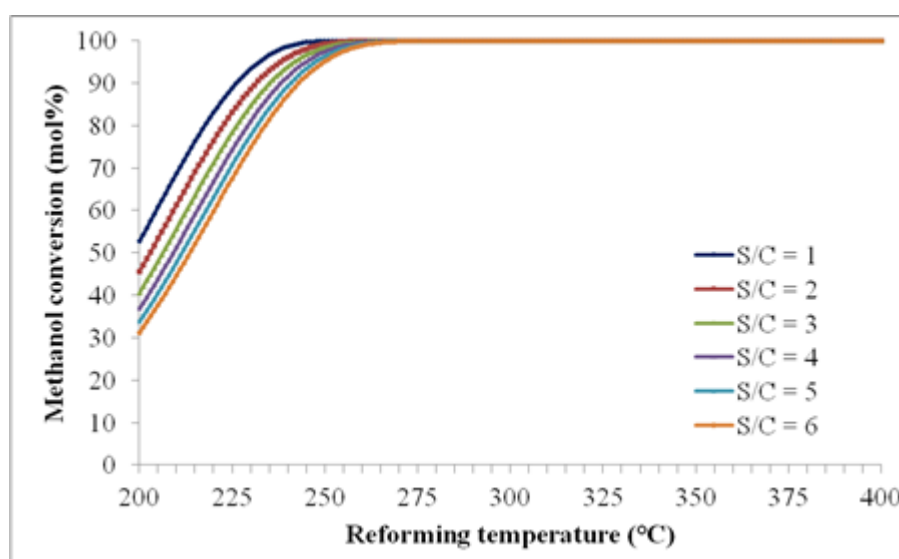

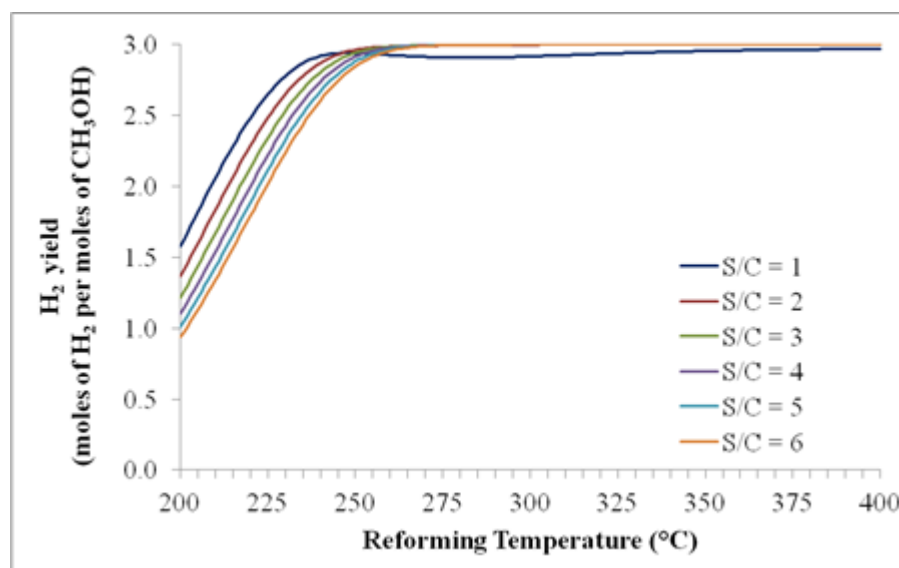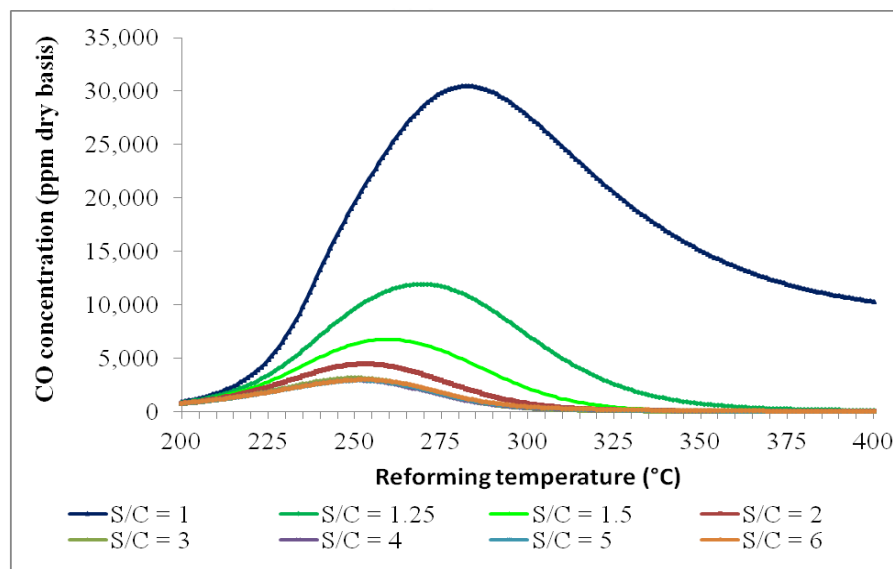Fig. 16   CO concentration as a function of reforming temperature and S/C feed ratio (Temperature = 200-400 °C, S/C = 1-6, CH_3OH = 2.5 mol/h, λ = 0.60)

5.2 Optimization of sorption-enhanced and conventional steam methanol reforming (SE-SMR and SMR)

The maximizing H_2 yield for the sorption-enhanced steam methanol reforming (SE-SMR) was performed in order to obtain the optimal condition compared with the conventional steam methanol reforming (SMR). Thus, the optimization of the SMR process was conducted based on maximum H_2 amount obtained from the SE-SMR process. The constraint for both systems was the limit of CO concentration in the final product at 10 ppm dry basis. Results for the optimization are shown in Table 12.

Table 12 Simulation results of sorption-enhanced and conventional steam methanol reforming (SE-SMR and SMR) under optimal operating conditions

Simulation results	SE-SMR Case I	SE-SMR Case II	SMR Case I	SMR Case II
Methanol feed inlet (mol/h)	2.50	2.50	2.50	2.50
Steam feed inlet (mol/h)	4.79	4.24	4.27	3.01
S/C feed ratio	1.92	1.70	1.71	1.20
Total steam feed inlet comparing to SMR process (%)	+ 12 (compared with SMR, Case I)	+ 41 (compared with SMR, Case II)	-	-
Reformer temperature (°C)	339	350	284	250
Net heat duty (kJ/h)**	+ 560.51	+ 534.03	+439.11	+ 378.77
Net heat duty comparing to SMR process (%)**	+ 28 (compared with SMR , Case I)	+ 41 (compared with SMR, Case II)	-	-
Methanol conversion (%)	100	100	100	99.99

** Net heat duty for SE-SMR included all heat input and output from the reactors (SE-SMR and REGEN) and the heat exchangers (H1, H2, H3, H4, H5, C1, and C2), referring to Figs. 17-18.
** Net heat duty for SMR included all heat input and output from the reactors (SMR, WGS, and PROX) and the heat exchangers (H1, H2, H3, H4, C1, C2, and C3), referring to Figs. 19-20.

Table 12   Simulation results of sorption-enhanced and conventional steam methanol reforming (SE-SMR and SMR) under optimal operating conditions (continued)

Simulation results	SE-SMR Case I	SE-SMR Case II	SMR Case I	SMR Case II
H_2 yield at outlet reformer	3.00	3.00	2.92	2.92
H_2 concentration in outlet product of the reformer (% dry basis)	99.99	99.99	74.49	74.55
H_2 concentration in final product (% dry basis)	99.99	99.99	74.98	74.99
CO concentration in final product (ppm dry basis)	10.00	9.89	0.00	0.00

Results from the optimization showed that the maximum H_2 yield for the sorption-enhanced steam methanol reforming (SE-SMR) was 3 moles H_2 per mole CH_3OH. In the optimization Case I, based on the same amount of H_2 in final product, S/C feed ratio for the SE-SMR was more than that obtained from the SMR about 12%. Higher steam flow rate for the SE-SMR was required to get the H_2 product with low CO concentration at less than 10 ppm. Results for the optimization, Case II were in the same way as Case I, S/C feed ratio for the SE-SMR was more than that obtained from the SMR about 41%. Results are in accord with Mahishi et al. (2008) that CO concentration was reduced by increasing steam-to-ethanol molar feed ratio based on the sorption-enhanced steam reforming of ethanol.

As shown in Table 12, the optimal reforming temperature for the SE-SMR, Case I was 339 °C and higher than the reforming temperature of the SMR, Case I at 284 °C. The optimal reforming temperature for the SE-SMR, Case II was 350 °C and higher than the reforming temperature of the SMR, Case II at 250 °C. In this optimization, reforming temperature of the SE-SMR process was higher than the SMR process because the SE-SMR must be operated at higher temperature to achieve

the better conversion of CaO and CO_2 influencing by the constraint of CO concentration at 10 ppm dry basis.

The heat input to each reformer under the optimal condition is presented in Figs. 17-20, the sorption-enhanced steam reformer released useful heat of 290.20 kJ/h for Case I and 289.16 kJ/h for Case II as the exothermic reaction of carbonation reaction are predominate over other reactions. Results are consistent with the study of Li et al. (2012) which reported that the sorption-enhanced steam reforming of methanol released heat from the reformer. Moreover, Mahishi et al. (2008) reported that the exothermic CO_2 absorption in the sorption-enhanced steam reforming of ethanol can supply heat to the endothermic ethanol reforming. Hence, the net external heat required by the reformer is reduced. The optimization showed that the conventional steam reformer required an external heat input of 158 kJ/h for Case I and 153.64 kJ/h for Case II due to the predominance of endothermic reactions of methanol steam reforming and methanol decomposition. Result complies the study of Lotric and Hocevar (2012), they indicated that the methanol steam reforming needed the sufficient heat to the process as it is proceeded by the endothermic reforming reaction. However, the net heat duty required by the SE-SMR processes in two cases were higher than the SMR processes due to the combustion unit for CaO regeneration and higher steam fed to the reactor. The higher amount of steam fed to the reactor leads to higher heat input required for the vaporizer H2 as presented in Figs. 17-18.

Although the total heat duty for the SE-SMR process is very high but there are lots of benefits as the following. H_2 purity from the SE-SMR process was very high at 99.99%, whereas H_2 purity leaving the preferential oxidation (PROX) reactor of the SMR process was 74.98-74.99%. The main reason for the low H_2 purity in the final

product produced by the SMR process is the remaining CO_2 component since there is no removal process of CO_2. With using a sorption-enhanced steam reformer, CO_2 can be removed leading to high H_2 purity product. Furthermore, product with very high purity of H_2 can be produced by a single sorption-enhanced steam reformer without any purification unit. The H_2 purity of 99.99% from the SE-SMR process is high enough to use with PEM fuel cell. To achieve product with high purity of H_2 by the SMR process, more separation units are required since the H_2 product from the SMR is in a low range of H_2 purity.

With the minimization of the net heat duty required for the SE-SMR process and the SMR process, result showed that the net heat duty required by the SE-SMR, Case II was 534.03 kJ/h which was less than the net heat duty required from the SE-SMR process, Case I at 560.51 kJ/h. The reduction in net heat duty required by the SE-SMR process, Case II was about 4.7% compared with Case I. The reduction of net heat duty required for the SE-SMR, Case II results from the reduction of steam fed to the reformer. As the heat required for vaporizing water is high due to the high heat of vaporization of water, an amount of water fed to the system is reduced leading to the slow reaction rate of water gas shift reaction. Consequently, higher reforming temperature is needed to enhance the carbonation reaction to achieve the low CO concentration at 10 ppm.

Based on the same amount of H_2 produced by the SE-SMR processes, Case I and Case II, the optimal condition from the SE-SMR process, Case II was selected to apply on the following study as the condition gave the advantage of lower external energy required. In the same way, the optimal condition from the SMR process, Case II was selected as the base case for comparing with the SE-SMR process in further

study. Figs. 17-20 show the simulation results for the SE-SMR processes, Case I, Case II and the SMR processes, Case I, Case II under optimal operating condition.
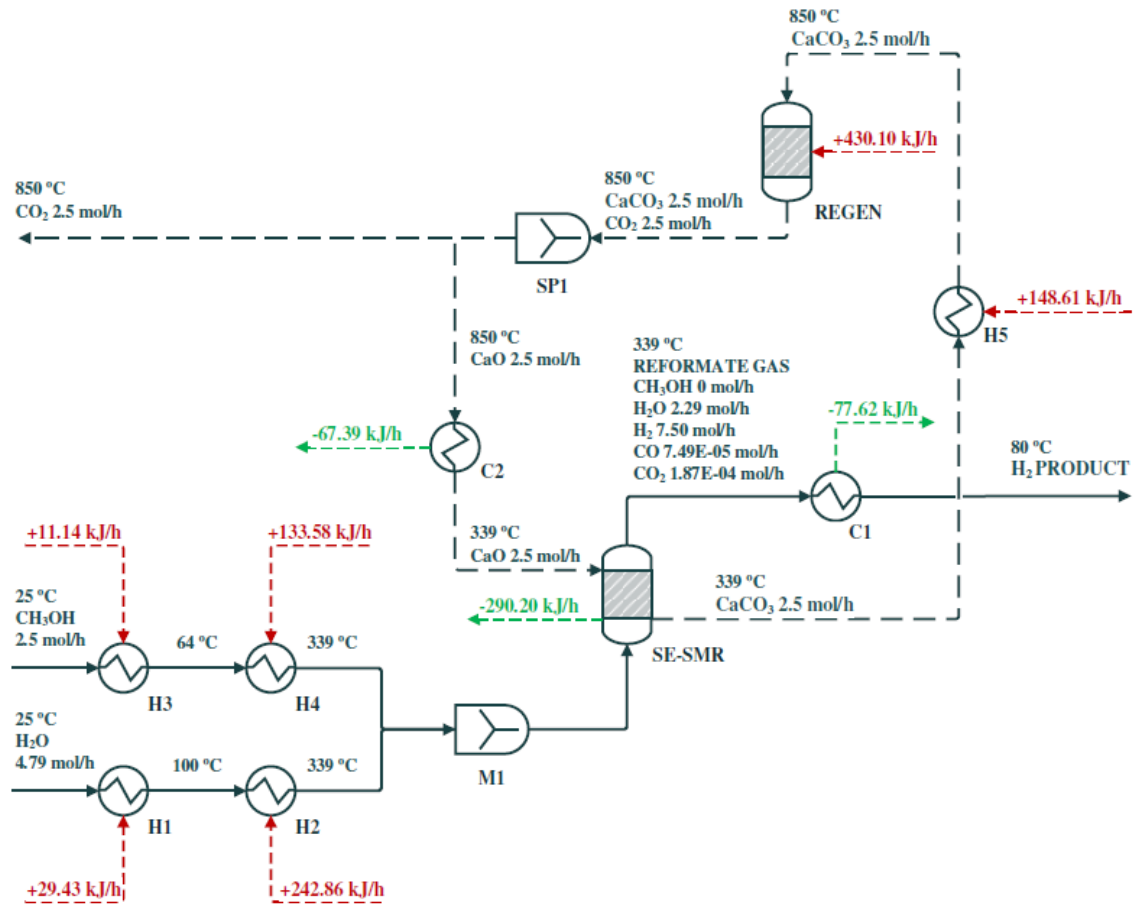
Fig. 17   Sorption-enhanced steam methanol reforming (SE-SMR) process

under optimal operating conditions, Case I
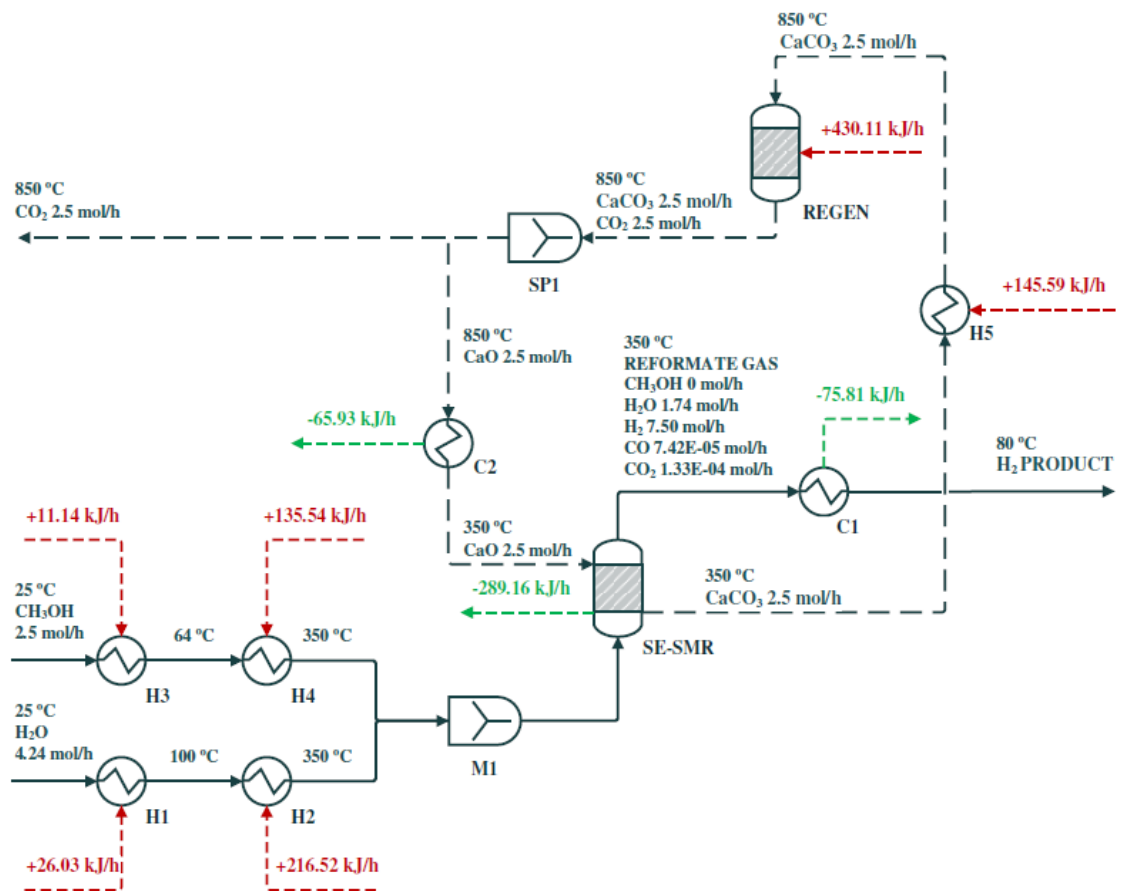
Fig. 18   Sorption-enhanced steam methanol reforming (SE-SMR) process

under optimal operating conditions, Case II
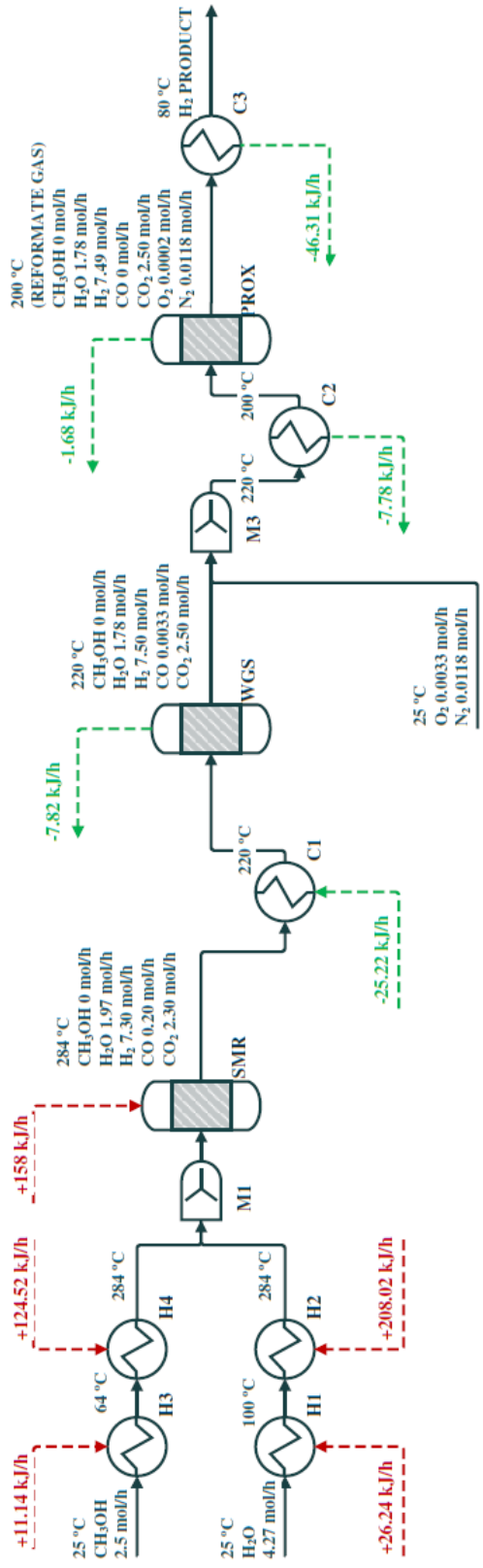
Fig. 19 Conventional steam methanol reforming (SMR) process

under optimal operating conditions, Case I
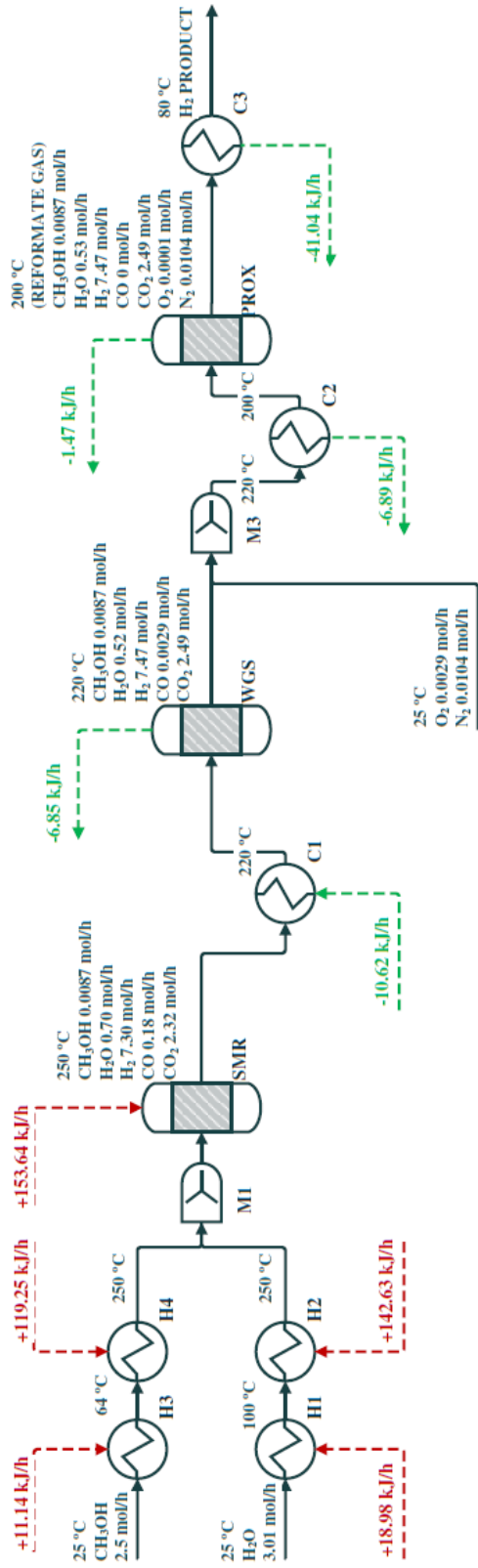
Fig. 20 Conventional steam methanol reforming (SMR) process

under optimal operating conditions, Case II

5.3 **Heat exchanger network design and thermal efficiency evaluation of sorption-enhanced steam methanol reforming (SE-SMR) process**

The improvement for the thermal efficiency and heat exchanger network design of the sorption-enhanced steam methanol reforming (SE-SMR) process were performed. To achieve a higher thermal efficiency of the process, heat duty required from external source shall be reduced as much as possible. Hence, the heat recovery within the process is necessary. The heat recovery of the SE-SMR process was determined by the composite hot and cold curves. The sources of heat and sink in terms of hot streams and cold streams were first identified from the material and energy balance illustrated in Fig. 18. The hot stream and cold stream identification is shown in Table 13. This table was used to create the composite hot and cold curves. However, the heat integration for this study was still in the preliminary stage.

Composite hot and cold curves were conducted by a T-Q diagram (temperature-enthalpy change diagram) which plotted the supply temperature and the target temperature of the stream in a y-axis versus the enthalpy change of the stream in an x-axis. This method focused on a temperature driving force for the heat transfer between the streams involving sensible heating and cooling of hot and cold streams as presented in Eqs. (37)-(38).

Hot stream: $\Delta H_H \left(\dfrac{kJ}{h} \right) = \left(\dot{M}\hat{C}_p \right)_H \left(\dfrac{kJ}{h \cdot {}^\circ C} \right)\left(T_H^{supply} - T_H^{target} \right)\left({}^\circ C \right)$ (37)

Cold stream: $\Delta H_C \left(\dfrac{kJ}{h} \right) = \left(\dot{M}\hat{C}_p \right)_C \left(\dfrac{kJ}{h \cdot {}^\circ C} \right)\left(T_C^{target} - T_C^{supply} \right)\left({}^\circ C \right)$ (38)

Where:

$\Delta H_{H,C}$ is total heat transferred from hot stream (H) or cold stream (C).

$\left(\dot{M}\hat{C}_p\right)_{H,C}$ is heat capacity rate of hot stream (H) or cold stream (C).

$T_{H,C}^{supply}$ is supply temperature (initial temperature) of hot stream (H) or cold stream (C).

$T_{H,C}^{target}$ is target temperature (final temperature) of hot stream (H) or cold stream (C).

For the heat transfer by vaporizing and condensing streams, a vaporizing stream and a condensing stream are changed to a cold stream and a hot stream, respectively by a 1 °C change and a heat capacity rate for the cold stream and the hot stream as presented in Eqs. (39)-(40). One degree Celsius is subtracted from the condensing stream temperature and 1 °C is added to the vaporizing stream temperature. By the different temperature of 1 °C, the heat capacity rates of the assumed cold and hot streams equal to the vaporization duty and condensation duty. This technique was applied to the vaporizing streams of water and methanol fed to the reformer. The heating of methanol feed stream and water feed stream were divided into three sections. First section was responsible for the feed stream heating from the room temperature of 25 °C to the boiling point of each feed stream, 100 °C for water and 64 °C for methanol. Secondly, heated water and methanol were vaporized and finally heated to the sorption-enhanced steam reforming temperature at 350 °C. Hence, the stream identification relying on Fig. 18 was replaced by the mentioned technique for the composite curve analyses in Fig. 21.

Vaporizing stream/Cold stream: $\left(\dot{M}\hat{C}_p\right)_C\left(\dfrac{kJ}{h\cdot°C}\right) = \dfrac{Q_C\left(\dfrac{kJ}{h}\right)}{1°C}$ (39)

Condensing stream/Hot stream: $\left(\dot{M}\hat{C}_p\right)_H\left(\dfrac{kJ}{h\cdot°C}\right) = \dfrac{Q_H\left(\dfrac{kJ}{h}\right)}{1°C}$ (40)

Where:

Q_C is the vaporization duty for the cold stream.

Q_H is the condensation duty for the hot stream.

Special consideration for additional heat exchange streams were made due to an attempt to find the most heat recovery. The additional heat recovery was conducted between process streams and waste heat utility streams. The considered waste heat utility stream involved the regeneration unit. High amount of heat required for this unit was obtained from the combustion of methane in a fired heater. Flue gas stream was occurred and left the fired heater after the combustion process. As the combustion reaction was operated at high temperature, the flue gas stream was left the fired heater at high temperature with high heat of enthalpy accordingly. Thus, it was considered as the waste heat utility stream and conducted the heat exchange to the other cold streams in the SE-SMR process enhancing the heat recovery in the system. A stoichiometric ratio of methane and oxygen in air feed stream for the combustion reaction (Eq. (41)) was employed to the system. The flue gas from the fired heater was assumed to be including of CO_2, H_2O and N_2 regarding the combustion reaction of methane in Eq. (41).

Combustion reaction of methane:

$$CH_4 + 2O_2 \rightarrow CO_2 + 2H_2O \tag{41}$$

Table 13   Hot and cold streams data extracted from the flowsheet, Fig. 18, for the composite curve analyses

Stream	Type	Supply temperature (°C)	Target temperature (°C)	Heat capacity rate (kJ/h.°C)	ΔH (kJ/h)
1. Flue gas from fired heater	Hot	860	265	0.252	150.03
2. Regenerated CaO cooling	Hot	850	350	0.082	65.93
3. H_2 product cooling	Hot	350	80	0.281	75.80
4. Methanol heating 1	Cold	25	64	0.286	11.14
5. Methanol vaporization	Cold	64	65	88.12	88.12
6. Methanol heating 2	Cold	65	350	0.166	47.42
7. H_2O heating 1	Cold	25	100	0.347	26.03
8. H_2O vaporization	Cold	100	101	172.16	172.16
9. H_2O heating 2	Cold	101	350	0.178	44.36
10. $CaCO_3$ heating	Cold	350	850	0.291	145.59

As seen in Table 13, the temperature of the flue gas was 860 °C based on the limitation of a minimum temperature difference (ΔTmin) at 10 °C comparing with the outlet process stream of the regeneration unit at 850 °C. The target temperature of the exhaust flue gas was expected at 265 °C. The heat capacity rate of the flue gas was determined from the heat and material balance of the regeneration system with the preheating of methane and air streams fed to the fired heater which will be explained in the following section.

The composite curves for the hot and cold streams in Table 13 were plotted on the same axes as shown in Fig. 21 to obtain the possible heat recovery amount within the system. Both composite curves for the hot and cold streams were set to have a minimum temperature difference (ΔTmin) of 10 °C. According to the composite curves, heat recovery was occurred from the hot stream composite curve to the cold stream composite curve vertically where the curves were overlapping. Fig. 21 showed the maximum heat recovery estimated from the composite curves, Q_{REC} was 266.81

kJ/h. Results showed that external heat utility was supplied to the extended cold stream composite curve as the heat recovery was not possible to occur. For this system, the external heat utility, Q_{Hmin} was 267.87 kJ/h excluding the external heat supply by the combustion of methane for the fired heater. The pinch temperature for the hot stream was 80 °C and the pinch temperature for the cold stream was 70 °C based on a minimum temperature difference (ΔTmin) of 10 °C.
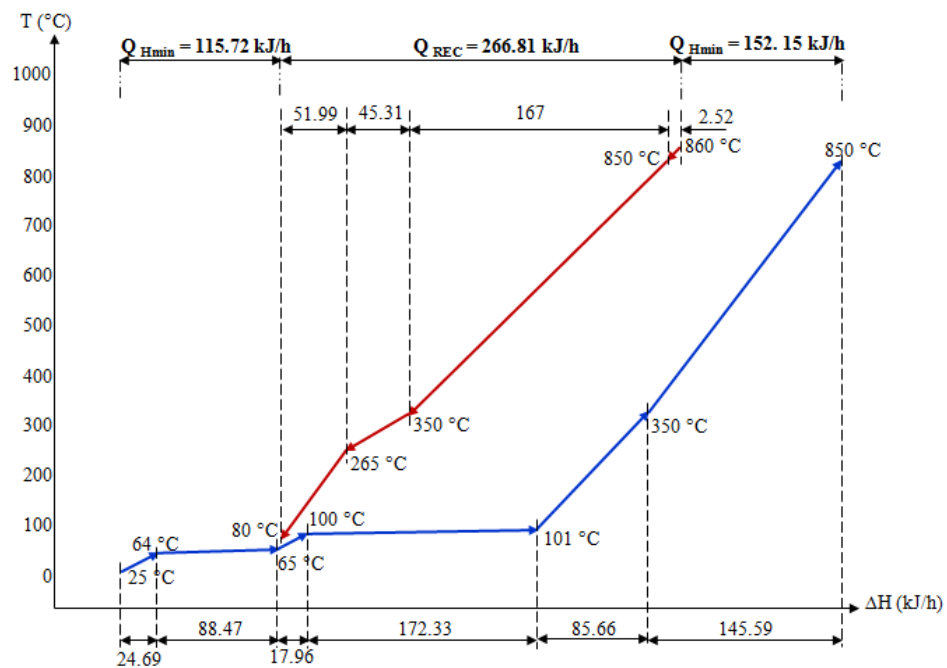
Fig. 21 The hot and cold composite curves plotted at ΔTmin = 10 °C

The heat exchanger network for the sorption-enhanced steam methanol reforming (SE-SMR) process corresponding the hot and cold composite curves in Fig. 21 was designed by the "tick-off" heuristic and the "grid diagram" (Smith a, 2005; Smith b, 2005) as presented by Fig. 22. The design of heat exchange between hot streams and cold streams was performed above pinch temperature, 80 °C for the hot stream and 70 °C for the cold stream, where the heat recovery was occurred. The heat

transfer was shown on the grid diagram; the heat transfer from the hot stream at the top to the cold stream at the bottom was represented by a pair of blue circles. The cold streams which were not in the heat recovery operation would rely on the external heat utility represented by a circle with an "H". Fig. 22 showed the hot utility required from external source at 152.10 kJ/h. This amount should equal to the Q_{Hmin} above the pinch in Fig. 21 at 152.15 kJ/h. The difference was from the rounding error during calculation.
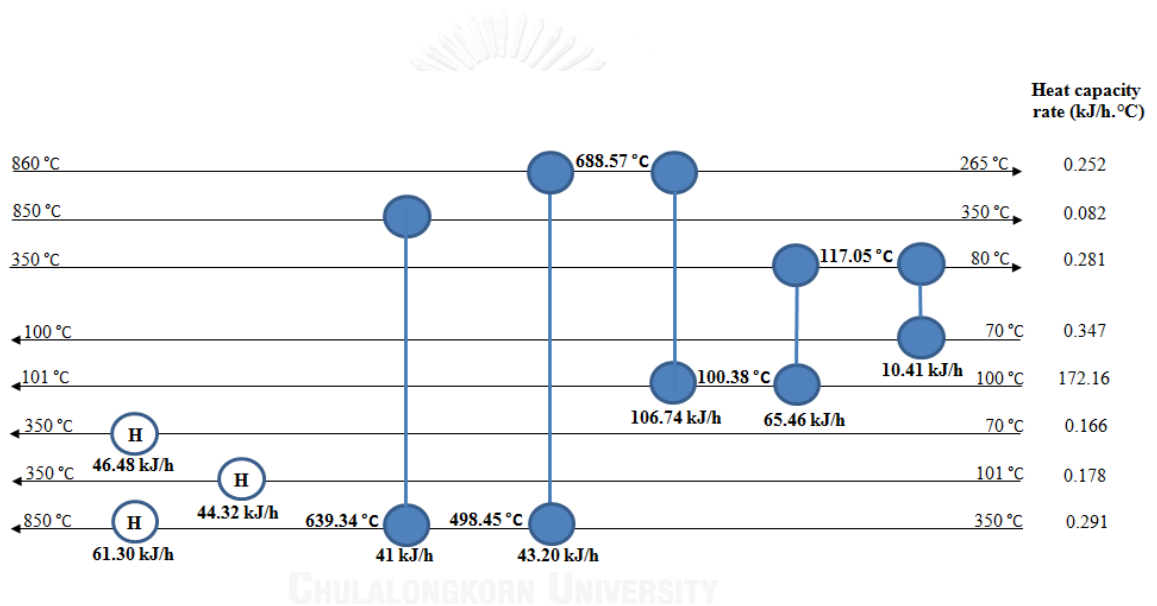
Fig. 22   Heat exchanger network design above pinch point on grid diagram

The process flow diagram of the sorption-enhanced steam methanol reforming (SE-SMR) process with the heat exchanger network design is explained in Fig. 23 for a better understanding. The heat exchangers with a red color represented the additional heat exchangers to be added in the process to achieve all heat recovery.

More one heat exchange stream was considered to minimize the heat utility required from an external source. As mentioned in the previous section, the sorption-enhanced steam reformer of methanol gave useful heat to the surrounding due to its

overall exothermic reaction. As the reformer was operated under isothermal condition, water cooling was required to maintain the reforming temperature at its condition. The starting temperature of the water cooling was assumed to be at 25 °C. The target of the water outlet temperature was set at 337 °C, 10 °C lower than the reforming temperature based on a minimum temperature difference (ΔTmin) of 10 °C. At this condition the water cooling became steam. The heat attained from the reformer was 289.16 kJ/h based on the process optimization Case II. With these given condition, the water cooling rate was determined at 0.092 kg/h. The heat of enthalpy available in this heated water cooling was used to preheat methane and air feed streams for the fired heater as illustrated in Fig. 24, to perform the heat recovery.

The preheating temperature of methane and air feed streams for the fired heater was assumed at 327 °C. The heat capacity rates of the streams and the heat duties of the preheaters were obtained from the heat and material balance of the regeneration unit, heat duty of methane preheater (PH-1) was 9.16 kJ/h and heat duty of air preheater (PH-2) was 59.16 kJ/h. The mass flow rates of methane and air feed streams for the fired heater are presented in Fig. 24. In this section, both of the heat transfer operations above and below pinch point were all considered.

As seen in Fig 24, the temperatures of steam from the methane preheater and air preheater were still high at 236.73 °C and 101.90 °C. Hence, it could be performed the heater recovery in other sections as presented in Fig. 24 to utilize the heat generated by the sorption-enhanced steam reformer as much as possible. Fig. 24 showed heat transferred from the steam to the methanol feed stream in heat exchangers H1-2 (a combination of H1-2 and H1-3, referring to Fig. 23) and H1, then heat from the steam transferred to the water feed stream in heat exchanger H3.
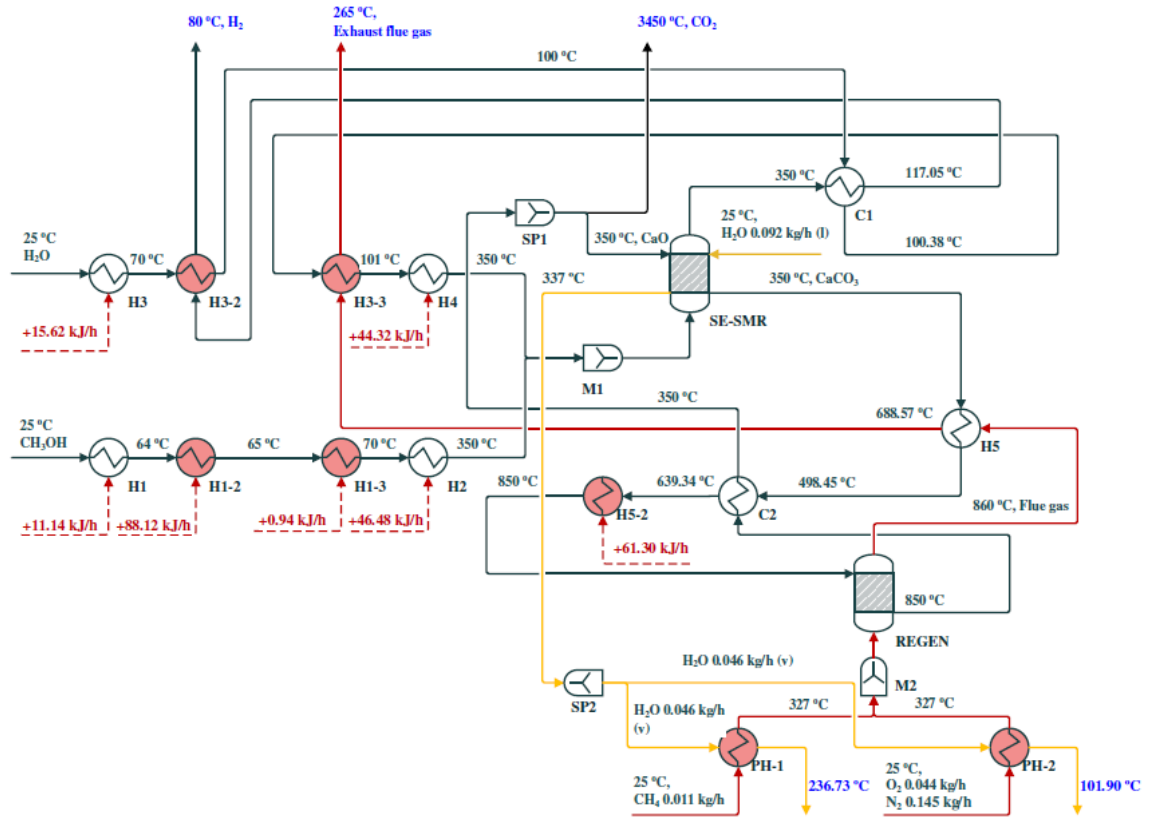
Fig. 23   Process flow diagram of SE-SMR process with

heat exchanger network design
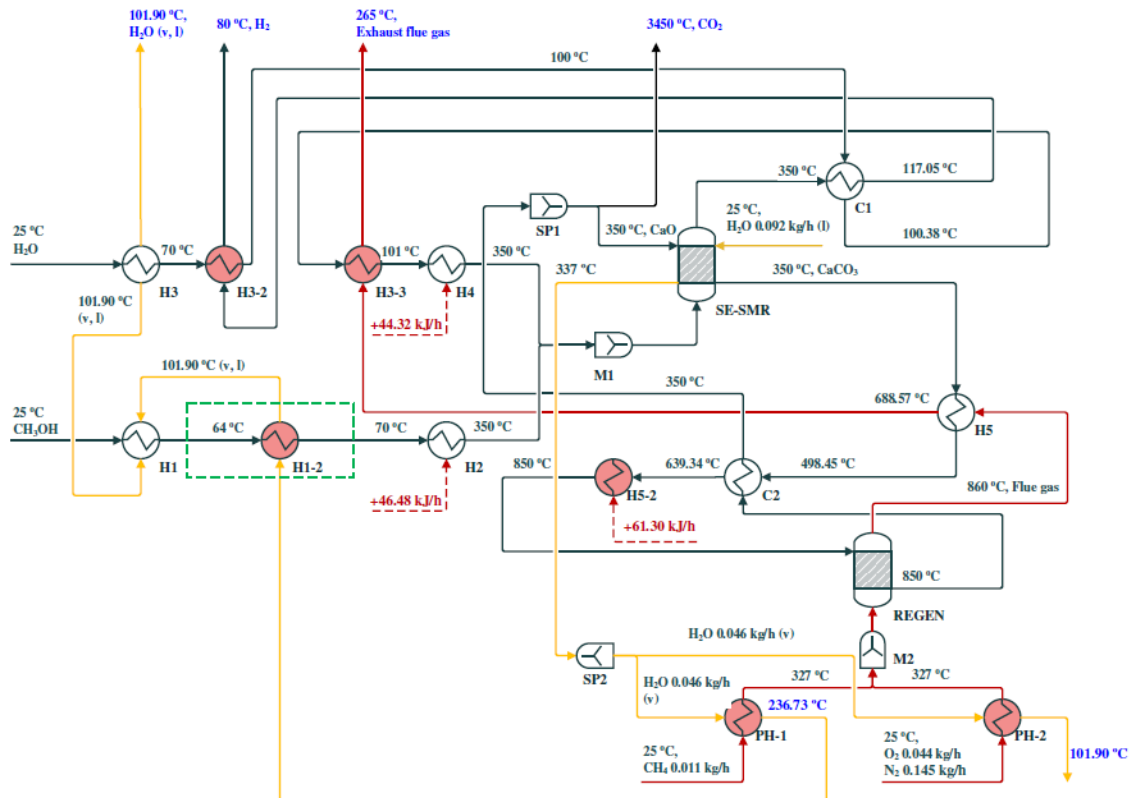
Fig. 24   Process flow diagram of SE-SMR process with

heat exchanger network design including heat integration for H1-2, H1, and H3

The heat recovery conclusion for the sorption-enhanced steam methanol

reforming (SE-SMR) process Case II was depicted in Table 14.

Table 14   The heat recovery conclusion for sorption-enhanced steam methanol reforming (SE-SMR) process

	ΔH (kJ/h)
Hot utility required before heat recovery operation	
Combustion via fired heater	548.41 kJ/h
Preheating for methane and air feed streams	68.32 kJ/h
Heating for cold process streams presented in Table 13	534.82 kJ/h
Total hot utility required before heat recovery operation	**1151.55 kJ/h**
Cold utility required before heat recovery operation	
Sorption-enhanced steam methanol reformer	289.16 kJ/h
Cooling for hot process streams presented in Table 13 (excluding the cooling of flue gas stream)	141.73 kJ/h
Total cold utility required before heat recovery operation	**430.89 kJ/h**
Heat recovery	
Heat recovery from hot and cold composite curves (including the flue gas stream)	266.81 kJ/h
Heat recovery from the reformer to preheat methane and air feed streams for the fired heater	68.32 kJ/h
Heat recovery from the reformer to heat exchangers H1-2, H1-3, H1, and H3	115.82 kJ/h
Total heat recovery	**450.95 kJ/h**
Cold utility required after heat recovery operation	
Sorption-enhanced steam methanol reformer	**289.16 kJ/h**
Hot utility required after heat recovery operation	
H_2O feed stream heater, H2	44.32 kJ/h
CH_3OH feed stream heater, H2	46.48 kJ/h
$CaCO_3$ heater, H5-2	61.30 kJ/h
Fired heater (combustion)	548.41 kJ/h
Total hot utility required after heat recovery operation	**700.51 kJ/h**

As shown in Table 14, the heat recovery rate of 450.95 kJ/h was about 39.16 % of the total hot utility required rate (1,151.55 kJ/h). Thermal efficiency of the SE-SMR process was evaluated by the equation developed by Mahishi et al (2008). The expressions for the thermal efficiency of the SE-SMR process are presented in Eqs.

(42)-(43) below. The lower heating value at 0 °C for hydrogen (LHV_{H2}), carbon monoxide (LHV_{CO}), and methanol (LHV_{CH3OH}) are 119,829 kJ/kg, 10,096 kJ/kg, and 21,111 kJ/kg (Aspen Plus Version 8.2., 2014), respectively.

$$\eta_{SE-SMR} = \frac{\text{Energy output}}{\text{Energy supplied}} \tag{42}$$

$$\eta_{SE-SMR} = \frac{\dot{m}_{H_2}LHV_{H_2} + \dot{m}_{CO}LHV_{CO}}{\dot{m}_{CH_3OH}LHV_{CH_3OH} + \text{External heat supplied}} \tag{43}$$

The thermal efficiency of the sorption-enhanced steam methanol reforming (SE-SMR) process, Case II with heat integration was compared to the conventional steam methanol reforming (SMR) process, Case II. Results are provided in Table 15.

Table 15   The comparison of thermal efficiency between SE-SMR process, Case II and SMR process, Case II

	SE-SMR Case II	SMR Case II
Energy output by product gas of H_2 and CO (kJ/h)	1,797.46	1,790.25
Energy input by methanol (kJ/h)	1,688.88	1,688.88
External heat supply (kJ/h)	700.51	445.64
Thermal efficiency (%)	**75.23**	**83.87**

Regarding the results in Table 15, the thermal efficiency of the SE-SMR process, Case II was about 75.23 % while 83.87% was achieved for the SMR process, Case II. Although the heat recovery was applied to the SE-SMR process but the thermal efficiency of the SE-SMR process was still less than that obtained from the SMR process due to the high external heat required for the regeneration unit.

As presented in Table 14, the external heat supply for the SE-SMR process before applying the heat recovery was 1,151.55 kJ/h, the thermal efficiency

determined by Eq. (43) was about 63.28%. Results showed that the heat recovery could improve the thermal efficiency as the thermal efficiency increased from 63.28% to 75.23%.

5.4   Economic analyses of sorption-enhanced steam methanol reforming (SE-SMR) process

The simplified profit estimation for hydrogen production by the sorption-enhanced steam methanol reforming (SE-SMR) process in terms of cost and revenue was proposed under the optimal conditions in Case II. Results are compared to the conventional steam methanol reforming (SMR) process, Case II based on the same amount of hydrogen product around 7.5 mol/h. The profit is defined by Eq. (44) below.

$$\text{Profit (\%)} = \frac{\text{Selling price of hydrogen - Cost of hydrogen production}}{\text{Selling price of hydrogen}} \times 100 \qquad (44)$$

The selling price of hydrogen was based on hydrogen produced by the reforming process at the on-site hydrogen filling station. Hydrogen usually sales as fuel supply for the fuel cell vehicles, its price was estimated at $13/kg at the fuel station (Hill & Penev, 2014). The cost of hydrogen production was the sum of a fixed cost and an operating cost, the fixed cost was rely on methanol steam reforming catalyst price at $20/kg (Alibaba.com., 2014), and limestone sorbent price at $0.025/kg (Harrison, 2008). The operating cost was based on methanol feed cost about $0.48/kg (Methanex, 2014), the amount of energy used in the production, and the compression cost for hydrogen supply at the fuel station. The cost of the energy was determined from the natural gas price at $5.21/mmBtu (Henry hub natural gas spot price, 2014 cite in QED environmental systems). The compression cost for hydrogen included the compression, storage, and dispensing (CSD) was about $1.88/kg (Bromaghim et al., 2010). Details of profit estimation for performing the economic analysis of hydrogen production by the SE-SMR process, Case II are presented in Table 16. It was compared with the profit from hydrogen production by the SMR process, Case II,

without heat integration which is presented in Table 17. One hour of the operation time was assumed for the economic analysis.

Table 16   Profit estimation of hydrogen production by SE-SMR process, Case II at hydrogen filling station

	Cost/unit	Capacity	Total cost / selling price
Fixed cost			
Catalyst	$20/kg catalyst	2.60×10^{-3} kg/h	5.20×10^{-2}/h
Limestone sorbent	$0.025/kg CaO	1.80×10^{-2} kg/h	4.50×10^{-4}/h
Operating cost			
CH_3OH feed	$0.48/kg CH_3OH	0.08 kg/h	3.84×10^{-2}/h
Natural gas price	$5.21/mmBtu	700.51 kJ/h (6.63×10^{-4} mmBtu/h)	0.35×10^{-2}/h
CSD cost	$1.88/kg H_2	0.015 kg/h	2.82×10^{-2}/h
Total production cost	-	-	12.26×10^{-2}/h
Selling price of H_2			
H_2 price at filling station	$13/kg H_2	0.015 kg/h	19.50×10^{-2}/h
		Profit	**37.13%**

Table 17   Profit estimation of hydrogen production by SMR process, Case II at hydrogen filling station

	Cost/unit	Capacity	Total cost / selling price
Fixed cost			
Catalyst	$20/kg catalyst	2.60×10^{-3} /h	5.20×10^{-2}/h
Limestone sorbent	-	-	-
Operating cost			
CH_3OH feed	$0.48/kg CH_3OH	0.08 kg/h	3.84×10^{-2}/h
Natural gas price	$5.21/mmBtu	445.64 kJ/h (4.22×10^{-4} /h mmBtu/h)	0.22×10^{-2}/h

Table 17   Profit estimation of hydrogen production by SMR process, Case II at hydrogen filling station (continued)

	Cost/unit	Capacity	Total cost / selling price
CSD cost	$1.88/kg H_2	0.015 kg/h	$2.82 x 10^{-2}/h
Total production cost	-	-	$12.08 x 10^{-2}/h
Selling price of H_2			
H_2 price at filling station	$13/kg H_2	0.015 kg/h	$19.50 x 10^{-2}/h
		Profit	**38.05%**

As illustrated in Tables 16-17, the profit of the SE-SMR process was 37.13% while the profit of 38.05% was achieved for the SMR process. The lower profit for the SE-SMR process results from the limestone sorbent cost and higher external utility supply cost which lead to higher cost of production.

As shown in Table 15, the feasibility of hydrogen production by the SE-SMR process tended to be more inferior than the SMR process in terms of the energy used as the hot utility required for the SE-SMR process was 700.51 kJ/h, higher than the SMR process at 445.64 kJ/h. But after performing the profit estimation, results showed the insignificant difference on the operating cost of both processes since the natural gas price was low and did not affect the operating cost for the SE-SMR process although its heat required was high. Thus, the hydrogen production by the SE-SMR process is competitive compared to the SMR process.

Hill and Penev (2014) reported that 1 kg of hydrogen equals to 3.3 gallon of gasoline. With the price of hydrogen at $13/kg, the hydrogen price was $3.94/gallon compared to the gasoline price. Independent Statistics and Analysis, U.S. Energy Information Administration (2014) reported the latest gasoline price in United States of America based on October 27, 2014 was at $3.06/gallon. Thus, the hydrogen target

price of \$13/kg was slightly expensive than the gasoline price. Hence, hydrogen is still attractive for the customer to use a hydrogen driven vehicle (Hill & Penev, 2014).

The economic analysis in this study was a preliminary study. The analysis discarded the cost of system design and construction, the cost of installation and permitting, the equipment expense, the cost of maintenance, and the cost of depreciation. Future work is suggested to perform the economic analysis including all involved parameters as mentioned to have an accurate total production cost. However, with regarding the equipment expense, the sorption-enhanced steam reforming process tended to be more competitive than the conventional steam reforming process as reported by Mahishi et al. (2008) and Hufton et al. (2000). Mahishi et al. (2008) reported that the sorption-enhanced steam reforming process leads to less equipment required, and hence, there is a possibility of reducing the capital cost. Hufton et al. (2000) reported that the key advantage of the sorption-enhanced steam reforming process is the reduction of pressure swing adsorption separation cost. By performing the economic analysis of the process design, the sorption-enhanced steam reforming process has the potential to reduce hydrogen production cost about 25% compared to the conventional steam reforming process (Hufton et al., 2000).

CHAPTER VI

CONCLUSION

The sensitivity analyses by the simulation of sorption-enhanced steam methanol reforming (SE-SMR) over $Cu/ZnO/Al_2O_3$ catalyst were performed to study the effect of process parameters to the performance of the hydrogen production. The RPlug model based on the kinetic rate expressions of methanol decomposition, methanol steam reforming, water gas shift reaction, and carbonation reaction were used to simulate the reforming process. The sensitivity analyses showed that the product distribution for the SE-SMR was greatly affected by the sorbent-to-catalyst volume ratio (λ), steam-to-methanol molar feed ratio (S/C feed ratio), and reforming temperature. To achieve high hydrogen purity with low CO concentration at less than 10 ppm molar dry basis in the final product stream and to limit reforming temperature below the degradable temperature of the catalyst at 350 °C, the sorbent-to-catalyst volume ratio was founded to be 0.60.

The SE-SMR was optimized to obtain the optimal operating condition for maximizing the hydrogen yield and minimizing the net heat duty required by the process with the CO concentration less than 10 ppm molar dry basis. For the maximization of hydrogen yield, Case I, the optimal condition for the SE-SMR was at the temperature of 339 ∘C with S/C feed ratio of 1.92. For the minimization of net heat duty required by the process, Case II, the optimal operating condition for the SE-SMR was at the temperature of 350 ∘C with S/C feed ratio of 1.70. At the same hydrogen yield, it is concluded from the optimization results from two cases that a reforming temperature is inversely proportional to a steam used for a reforming, lower

amount of steam leads to higher reforming temperature. Under the optimal condition of the SE-SMR and the SMR in Case I and Case II, the use of sorbent was proven to be able to increase the hydrogen yield based on the hydrogen product from the reformers. This enhancement increased the final hydrogen concentration from 74.98-74.99% to 99.99% on gas product in molar dry basis.

With regard to the optimization of the SE-SMR in Case II, the net heat duty required by the process was reduced about 4.7% with respect to the optimization in Case I due to the lower steam amount. If the sorption-enhanced steam reforming of methanol can be operated in the temperature over 350 °C, steam amount can be reduced and the reforming process can be operated with a lower net heat duty required.

Comparing to the conventional steam methanol reforming (SMR) process with the optimization, the SE-SMR process was better in terms of the high hydrogen purity product of 99.99% without any purification unit as the almost 100% removal of CO_2 by the sorbent shifted the equilibrium of reaction in favor of hydrogen. The SE-SMR was found to be operated at higher temperature and S/C feed ratio based on the same specification of hydrogen product. The net heat duty required for the SE-SMR process was higher than the SMR process about 27% based on the optimization Case I and 41% based on the optimization Case II due to the higher amount of steam fed to the reformer and the combustion unit for CaO regeneration. Hence, the SE-SMR process might not be worthwhile in terms of heat required for the reforming process. However, there was a room for improvement. The recommendation was to perform heat integration or heat recovery for the SE-SMR process to attain a lower heat required by the process.

The disadvantage of the SE-SMR process was occurred from the high heat duty required by the process. The heat integration by the pinch analysis was performed to determine heat recovery within the process streams and the waste heat utility streams, and to design the heat exchanger network. After the heat integration, the heat recovery of the SE-SMR process was determined at 39.16 % of the total energy that were used as hot utility supply to the overall process. By the heat integration operation, the thermal efficiency of the SE-SMR process increased from 63.28% to 75.23% due to the reduction of external heat required by the process. Although the thermal efficiency of the SE-SMR process was improved but it was still lower than the thermal efficiency of the SMR process at 83.87%. Thus, the simple economic analysis by the profit determination was performed to confirm the feasibility of the SE-SMR process. The studies showed the profit of the SE-SMR process was about 37.13% while the profit of the SMR process was obtained at 38.05%. As the difference of the profits are small and considered insignificance, the possibility of hydrogen product by the SE-SMR process is competitive compared to the SMR process. Even though the heat utility required for the SE-SMR process was much higher than the SMR process, the small difference of the determined profits was achieved since the price of natural gas as energy source was not expensive.

The sorption-enhanced steam reforming process is a potential innovation for producing high purity product of hydrogen. Higher hydrogen yield is achieved by the use of sorbent to remove CO_2 concentration. The sorption-enhanced steam reforming process can reduce CO_2 emission as there is a CO_2 removal function by the CaO sorbent. The hydrogen product can be produced with very small content of CO_2 component. Carbon dioxide is later released from the sorbent through the regeneration

unit. The desorbed CO_2 in a very high purity will be easily captured and utilized in other application. Hence, the CO_2 emission is reduced. The complexity of the conventional steam reforming process is minimized by the sorption-enhanced steam reforming process since it can produce high purity grade of hydrogen with a single reformer resulting in lesser equipment required by the process. For this reason, the capital and maintenance cost for the process are possible to be reduced compared to the conventional stem reforming. With the optimization and heat integration of the sorption-enhanced steam methanol reforming process, the competitiveness of the sorption-enhanced steam methanol reforming process is arisen compared to the conventional process.

REFERENCES

Alibaba.com. (2014). RYF104 type methanol steam reforming catalyst. Retrieved December 14, 2014, from http://www.alibaba.com/product-detail/RYF104-type-Methanol-steam-reforming-catalyst_1463197766.html

Alternative Fuels Data Center. U.S. Department of Energy. (2014). Fuel properties comparison. Retrieved September 19, 2014, from http://www.afdc.energy.gov/fuels/fuel_properties.php

Aspen Plus Version 8.2. (2014). Aspen Plus help: Aspen Technology, Inc. .

Bromaghim, G., Gibeault, K., Serfass, J., Serfass, P., & Wagner, E. (2010). Hydrogen and fuel cells: The U.S. market report: Technology Transition Corporation for the National Hydrogen Association.

Chang, B. K., & Tatarchuk, B. J. (2003). Preferential catalytic oxidation (PROX) of CO from model reformates for PEM fuel cells. Prepr. Pap.-Am. Chem. Soc., Div. Fuel Chem, 48(2).

Chao, Z., Wang, Y., Jakobsen, J. P., Fernandino, M., & Jakobsen, H. A. (2011). A turbulent Eulerian multi-fluid reactive flow model and its application in modelling sorption enhanced steam methane reforming. Journal of Physics, Conference series 318.

Choi, Y., & Stenger, H. G. (2003). Water gas shift reaction kinetics and reactor modeling for fuel cell grade hydrogen. Journal of Power Sources, 124, 432-439.

Choi, Y., & Stenger, H. G. (2005). Kinetics, simulation and optimization of methanol steam reformer for fuel cell applications. Journal of Power Sources, 142, 81-91.

Ding, Y., & Alpay, E. (2000). Adsorption-enhanced steam-methane reforming. Chemical engineering science, 55, 3929-3940.

Dybkjaer, I. (1995). Tubular reforming and autothermal reforming of natural gas-an overview of available processes. Fuel Processing Technology, 42, 85-107.

Feole, M. (2013). Modeling calcination in a rotary kiln using aspen plus. (Thesis submission).

Ghasemzadeh, K., Liguori, S., Morrone, P., Iulianelli, A., Piemonte, V., Babaluo, A. A., & Basile, A. (2013). H_2 production by low pressure methanol steam reforming in a dense Pd-Ag membrane reactor in co-current flow configuration: Experimental and modeling analysis. International Journal of Hydrogen Energy, 1-13.

Gockenbach, M. S. (2003). Introduction to sequential quadratic programming. Retrieved December 6, 2014, from http://www.math.mtu.edu/~msgocken/ma5630spring2003/lectures/sqp1/sqp1/node1.html

Harrison, D. P. (2008). Calcium enhanced H2 production with CO_2 capture. Sildes. Department of Chemical Engineering. Louisiana State University.

Hill, P., & Penev, M. (2014). Hydrogen fueling station in Honolulu, Hawaii feasibility analysis: U.S. Department of Energy National Laboratory operated by Battelle Energy Alliance.

Hoppe, R. H. W. (2006). Sequential quadratic programming, Optimization I, Chapter 4. Retrieved December 6, 2014, from http://www.math.uh.edu/~rohop/fall_06/

Hufton, J., Waldron, W., Weigel, S., Rao, M., Nataraj, S., & Sircar, S. (2000). Air Products and Chemicals,and others. Sorption enhanced reaction process (SERP) for the production of hydrogen. Paper presented at the The 2000 Hydrogen Program Review.

Independent Statistics and Analysis. U.S. Energy Information Administration. (2014). U.S. regular gasoline prices. Retrieved October 27, 2014, from http://www.eia.gov/petroleum/gasdiesel/

Johnson, K., Grace, J. R., Elnashaie, S. S. E. H., Kolbeinsen, L., & Eriksen, D. (2006). Modeling of sorption-enhanced steam reforming in a dual fluidized bubbling bed reactor. Industrial and Engineering Chemistry Research, 45, 4133-4144.

Katiyar, N., Kumar Shashi, & Kumar Surendra. (2013). Comparative thermodynamic analysis of adsorption, membrane and adsorption-membrane hybrid reactor systems for methanol steam reforming. International Journal of Hydrogen Energy, 38, 1363-1375.

Laumer, J. (2006). The official Chinese liquid transportation fuel of the future]. Retrieved September 19, 2014, from http://www.treehugger.com/cars/ methanol-the-official-chinese-liquid-transportation-fuel-of-the-future.html

Lee, D. K., Baek, H., & Yoon, W. L. (2004). Modeling and simulation for the methane steam reforming enhanced by in situ CO_2 removal utilizing the CaO carbonation for H_2 production. Chemical Engineering Science, 59, 931-942.

Lee, J. K., Ko, J. B., & Kim, D. H. (2004). Methanol steam reforming over $Cu/ZnO/Al_2O_3$ catalyst: kinetics and effectiveness factor. Applied Catalysis A, General 278, 25-35.

Levenspiel, O. (1999). Chemical reaction engineering, Third edition

Li, M., Duraiswamy, K., & Knobbe, M. (2012). Adsorption enhanced steam reforming of methanol for hydrogen generation in conjunction with fuel cell: Process design and reactor dynamics. Chemical Engineering Science, 67, 26-33.

Lotric, A., & Hocevar, S. (2012). Methanol steam reformer-high temperature PEM fuel cell system analysis. Military Green.

Mahishi, M. R., Sadrameli, M. S., Vijayaraghavan, S., & Goswami, D. Y. (2008). A novel approach to enhance the hydrogen yield of biomass gasification using CO_2 sorbent. ASME.

Martavaltzi, C. S., Pefkos, T. D., & Lemonidou, A. A. (2011). Operational window of sorption enhanced steam reforming of methane over $CaO-Ca_{12}Al_{14}O_{33}$. Industrial and Engineering Chemistry Research, 50, 539-545.

Martinez, V. C., Bretado, M. E., Zaragoza, M. M., Gutie´rrez, J. S., Ortiz, A. L., & (2013). Absorption enhanced reforming of light alcohols (methanol and ethanol) for the production of hydrogen: Thermodynamic modeling. International Journal of Hydrogen Energy, 38, 12539-12553.

Methanex. (2014). Methanex methanol price sheet. Retrieved August 30, 2014, from https://www.methanex.com/our-business/pricing

Mostafavi, E., Sedghkerdar, M. H., & Mahinpey, M. (2013). Thermodynamic and kinetic study of CO2 capture with calcium based sorbents: Experiments and modeling. Industrial and Engineering Chemistry Research 52, 4725-4733.

Nijmeijer, A. (1999). Hydrogen-selective silica membranes for use in membrane steam reforming. (Thesis), University of Twente, Enschede, Netherlands.

Ogden, J. M. (2001). Review of small stationary reformers for hydrogen production: Center of Energy and Environmental Studies, Princeton University.

Pajaie, H. S., Taghizadeh, M., & Eliassi, A. (2012). Hydrogen production from methanol steam reforming over $Cu/ZnO/Al_2O_3/CeO_2/ZrO_2$ nanocatalyst in an adiabatic fixed-bed reactor. Iranica Journal of Energy & Environment 3, (4), 307-313.

Peng, Z. (2003). A novel hydrogen and oxygen generation system. (Master of Science in Chemical Engineering Master Thesis), B.E., Tianjin University, 1995.

Peppley, B. A., Amphlett, J. C., Kearns, L. M., & Mann, R. F. (1999). Methanol-steam reforming on $Cu/ZnO/Al_2O_3$ catalysts. Part 2. A comprehensive kinetic model. Applied Catalysis A General 179, 31-49.

Phromprasit, J., Powell, J., Arpornwichanop, A., Rodrigues, A. E., & Assabumrungrat, S. (2013). Hydrogen production from sorption enhanced biogas steam reforming using Nickel-Based catalysts. Engineering Journal, Volume 17(Issue 4), 20-34.

Posada, A., & Manousiouthakis, V. (2005). Heat and power integration of methane reforming based hydrogen production. Industrial and Engineering Chemistry Research, 44, 9113-9119.

Purnama, H. (2003). Catalytic study of copper based catalysts for steam reforming of methanol. (Doctor of Engineering), Technical University of Berlin.

QED Environmental Systems. Henry hub natural gas spot price. Retrieved October 16, from http://www.qedenv.com/Applications/Landfill_Gas_Calculator/Methane _ Value

Rashidi, N. A., Rashidi, N. A., Mohamed, M., & Yusup, S. (2012). The kinetic model of calcination and carbonation of anadara granosa. International Journal of Renewable Energy Research, Vol. 2, No. 3.

Sa, S., Silva, H., Sousa, J. M., & Mendes, A. (2009). Hydrogen production by methanol steam reforming in a membrane reactor: Palladium vs carbon molecular sieve membranes. Journal of Membrane Science, 339, 160-170.

Sa, S. T. (2011). Methanol steam reforming for fuel cell applications. (Doctor in Chemical and Biological Engineering Doctor in Chemical and Biological Engineering), University of Porto.

Sanchez, R. A., Chao, Z., Solsvik, J., & Jakobsen, H. A. (2012). One dimensional two-fluid model simulations of the SE-SMR process operated in a circulating fluidized bed reactor. Procedia Engineering, 42, 1282-1291.

Sedghkerdar, M. H., Mostafavi, E., & Mahinpey, N. (2014). Investigation of the kinetics of carbonation reaction with CaO-based sorbents using experiments and Aspen plus simulation. Taylor and Francis.

Sivalingam, S. (2012). CO_2 separation by calcium looping from full and partial fuel oxidation processes. (Doctor-Engineer approved dissertation), The Technische Universität München.

Smith a, R. (2005) Chemical Process Design and Integration.

Smith b, R. (2005) Chemical Process Design and Integration.

Sun, P., Grace, J. R., Lim, C. J., & Anthony, E. J. (2008). Determination of intrinsic rate constants of the $CaO–CO_2$ reaction. Chemical Engineering Science, 63, 47-56.

Telotte, J. C., Kern, J., & Palanki, S. (2008). Miniaturized methanol reformer for fuel cell powered mobile applications.. International Journal of Chemical Reactor Engineering, Vol. 8, Article A64.

Tesser, R., Serio, M. D., & Santacesaria, E. (2009). Methanol steam reforming: A comparison of different kinetics in the simulation of a packed bed reactor. Chemical Engineering Journal, 154, 69-75.

Tzanetis, K. F., Martavaltzi, C. S., & Lemonidou, A. A. (2012). Comparative exergy analysis of sorption enhanced and conventional methane steam reforming. International Journal of Hydrogen Energy, 37, 16308-16320.

Vadlamudi, V. K., & Palanki, S. (2011). Modeling and analysis of miniaturized methanol reformer for fuel cell powered mobile applications. International Journal of Hydrogen Energy, 36, 3364-3370.

Vicente, J., Remiro, A., Atutxa, A., Ereña, J., Gayubo, A. G., & Bilbao, J. In situ capture of CO_2 in the steam reforming of ethanol over Ni/SiO_2 catalyst for hydrogen production.

Wesenberg, M. H. (2006). Gas heated steam reformer modelling. (Doctor Thesis), Norwegian University of Science and Technology.

Wu, W., Liou, Y., & Zhou, Y. (2012). Multiobjective optimization of a hydrogen production system with low CO_2 emissions. Industrial and Engineering Chemistry Research, 51, 2644-2651.

Xu, J., & Froment, G. F. (1989). Steam reforming, methanation and water-gas shift: I. Intrinsic kinetics. AIChE, J 35, 88-96.

Yunus, M. K., Ahmad, M. M., Inayat, A., & Yusup, S. (2010). Simulation of enhanced biomass gasification for hydrogen production using iCON. World Academy of Science, Engineering and Technology, Vol. 4.

APPENDIX

SIMULATED DATA

Table A1   CO concentration (ppm dry basis) based sorbent-to-catalyst volume ratio
(λ) of 0.4 (Temperature = 200-400 °C, S/C = 1, CH_3OH = 2.5 mol/h)

TEMP °C	H_2 OUT MOL/HR	CO_2 OUT MOL/HR	CO OUT MOL/HR	CO CONCENTRATION PPM DRY BASIS
200	3.9469	0.2170	0.0039	934.0114
210	5.1435	0.2290	0.0094	1755.7352
220	6.2015	0.2042	0.0225	3506.8315
230	6.9417	0.1440	0.0516	7235.9568
240	7.2923	0.0716	0.1031	13808.2851
250	7.3399	0.0260	0.1539	20468.1574
260	7.3041	0.0153	0.1953	25986.1992
270	7.2731	0.0171	0.2263	30112.2327
280	7.2592	0.0212	0.2404	31961.0738
290	7.2628	0.0238	0.2368	31479.0486
300	7.2785	0.0240	0.2212	29401.7648
310	7.2995	0.0222	0.2003	26629.8594
320	7.3208	0.0197	0.1790	23807.4161
330	7.3401	0.0171	0.1598	21262.3613
340	7.3563	0.0147	0.1436	19108.6472
350	7.3696	0.0128	0.1304	17352.2749
360	7.3801	0.0112	0.1198	15956.0483
370	7.3883	0.0099	0.1117	14871.9617
380	7.3945	0.0089	0.1055	14053.5546
390	7.3989	0.0081	0.1011	13460.4015
400	7.4019	0.0075	0.0980	13059.4574

Table A2   CO concentration (ppm dry basis) based sorbent-to-catalyst volume ratio
(λ) of 0.4 (Temperature = 200-400 °C, S/C = 2, CH_3OH = 2.5 mol/h)

TEMP °C	H_2 OUT MOL/HR	CO_2 OUT MOL/HR	CO OUT MOL/HR	CO CONCENTRATION PPM DRY BASIS
200	3.4181	0.2780	0.0028	746.4472
210	4.5873	0.3131	0.0058	1176.6491
220	5.7188	0.3105	0.0112	1848.2518
230	6.6214	0.2616	0.0192	2782.6597
240	7.1737	0.1807	0.0280	3788.8639
250	7.4045	0.1029	0.0332	4403.5394
260	7.4619	0.0551	0.0321	4248.2217
270	7.4740	0.0343	0.0259	3431.3716
280	7.4822	0.0245	0.0177	2358.9580
290	7.4895	0.0174	0.0105	1400.2405
300	7.4944	0.0115	0.0056	741.0003
310	7.4972	0.0071	0.0028	370.2893
320	7.4986	0.0041	0.0014	186.4115
330	7.4993	0.0024	0.0007	98.5906
340	7.4996	0.0014	0.0004	55.3648
350	7.4998	0.0008	0.0002	32.9129
360	7.4998	0.0005	0.0002	20.6360
370	7.4999	0.0003	0.0001	13.6986
380	7.4999	0.0002	0.0001	9.7631
390	7.4999	0.0002	0.0001	7.6839
400	7.4999	0.0001	0.0001	6.9313

Table A3   CO concentration (ppm dry basis) based sorbent-to-catalyst volume ratio
(λ) of 0.4 (Temperature = 200-400 °C, S/C = 3, CH_3OH = 2.5 mol/h)

TEMP °C	H_2 OUT MOL/HR	CO_2 OUT MOL/HR	CO OUT MOL/HR	CO CONCENTRATION PPM DRY BASIS
200	3.0458	0.3222	0.0024	720.3386
210	4.1743	0.3799	0.0049	1073.6728
220	5.3295	0.4020	0.0091	1577.9938
230	6.3265	0.3715	0.0149	2221.5587
240	7.0107	0.2918	0.0209	2853.7064
250	7.3516	0.1930	0.0238	3147.0802
260	7.4607	0.1134	0.0215	2832.6906
270	7.4834	0.0670	0.0156	2057.0905
280	7.4906	0.0424	0.0094	1239.7219
290	7.4951	0.0273	0.0049	652.7288
300	7.4975	0.0171	0.0025	326.2439
310	7.4987	0.0105	0.0013	169.9359
320	7.4993	0.0064	0.0007	95.9042
330	7.4996	0.0039	0.0004	57.6289
340	7.4997	0.0023	0.0003	35.9898
350	7.4998	0.0014	0.0002	23.0592
360	7.4999	0.0009	0.0001	15.1084
370	7.4999	0.0006	0.0001	10.1668
380	7.4999	0.0004	0.0001	7.1322
390	7.5000	0.0003	0.0000	5.3809
400	7.5000	0.0002	0.0000	4.5808

Table A4   CO concentration (ppm dry basis) based sorbent-to-catalyst volume ratio
(λ) of 0.6 (Temperature = 200-400 °C, S/C = 1, CH$_3$OH = 2.5 mol/h)

TEMP °C	H$_2$ OUT MOL/HR	CO$_2$ OUT MOL/HR	CO OUT MOL/HR	CO CONCENTRATION PPM DRY BASIS
200	3.9484	0.1546	0.0038	917.1711
210	5.1473	0.1590	0.0090	1698.8630
220	6.2076	0.1361	0.0214	3362.6516
230	6.9489	0.0892	0.0491	6930.1219
240	7.2997	0.0378	0.0986	13255.8977
250	7.3477	0.0103	0.1467	19545.5299
260	7.3138	0.0072	0.1856	24720.2533
270	7.2844	0.0101	0.2151	28643.7413
280	7.2711	0.0135	0.2285	30408.4881
290	7.2751	0.0154	0.2245	29874.3484
300	7.2914	0.0154	0.2083	27714.3735
310	7.3133	0.0142	0.1865	24823.5869
320	7.3356	0.0123	0.1643	21868.0029
330	7.3557	0.0105	0.1442	19195.1258
340	7.3728	0.0089	0.1271	16926.9254
350	7.3868	0.0076	0.1131	15068.8118
360	7.3980	0.0065	0.1019	13579.3926
370	7.4069	0.0057	0.0931	12405.2817
380	7.4137	0.0050	0.0863	11495.5708
390	7.4189	0.0045	0.0811	10806.4090
400	7.4227	0.0041	0.0773	10302.3010

Table A5   CO concentration (ppm dry basis) based sorbent-to-catalyst volume ratio
(λ) of 0.6 (Temperature = 200-400 °C, S/C = 2, CH_3OH = 2.5 mol/h)

TEMP °C	H_2 OUT MOL/HR	CO_2 OUT MOL/HR	CO OUT MOL/HR	CO CONCENTRATION PPM DRY BASIS
200	3.4188	0.2027	0.0027	748.2554
210	4.5893	0.2218	0.0056	1162.0475
220	5.7226	0.2114	0.0107	1792.8101
230	6.6265	0.1676	0.0180	2645.6489
240	7.1788	0.1050	0.0257	3520.1671
250	7.4091	0.0513	0.0298	3977.0764
260	7.4663	0.0235	0.0279	3705.2055
270	7.4783	0.0143	0.0215	2865.3057
280	7.4861	0.0104	0.0139	1854.6409
290	7.4925	0.0071	0.0075	1002.9058
300	7.4966	0.0042	0.0034	457.6197
310	7.4986	0.0022	0.0014	183.1056
320	7.4995	0.0010	0.0005	68.7568
330	7.4998	0.0005	0.0002	26.1329
340	7.4999	0.0002	0.0001	10.6087
350	7.5000	0.0001	0.0000	4.7296
360	7.5000	0.0001	0.0000	2.4002
370	7.5000	0.0000	0.0000	1.5099
380	7.5000	0.0000	0.0000	1.3199
390	7.5000	0.0000	0.0000	1.6043
400	7.5000	0.0001	0.0000	2.3721

Table A6   CO concentration (ppm dry basis) based sorbent-to-catalyst volume ratio (λ) of 0.6 (Temperature = 200-400 °C, S/C = 3, CH_3OH = 2.5 mol/h)

TEMP °C	H_2 OUT MOL/HR	CO_2 OUT MOL/HR	CO OUT MOL/HR	CO CONCENTRATION PPM DRY BASIS
200	3.0461	0.2426	0.0024	730.5574
210	4.1755	0.2777	0.0048	1077.8122
220	5.3321	0.2827	0.0088	1560.9428
230	6.3304	0.2474	0.0142	2155.5002
240	7.0150	0.1786	0.0195	2700.3504
250	7.3554	0.1036	0.0215	2878.5919
260	7.4641	0.0510	0.0186	2469.5694
270	7.4865	0.0257	0.0126	1672.4364
280	7.4932	0.0147	0.0068	906.2782
290	7.4970	0.0085	0.0030	402.7195
300	7.4988	0.0046	0.0012	155.2427
310	7.4996	0.0023	0.0004	57.9565
320	7.4998	0.0011	0.0002	23.3436
330	7.4999	0.0005	0.0001	10.4377
340	7.5000	0.0003	0.0000	5.0602
350	7.5000	0.0001	0.0000	2.6193
360	7.5000	0.0001	0.0000	1.4758
370	7.5000	0.0001	0.0000	0.9758
380	7.5000	0.0000	0.0000	0.8520
390	7.5000	0.0001	0.0000	1.0155
400	7.5000	0.0001	0.0000	1.4843

VITA

Jantawan Vungvira was born on the 8th of March, 1987 in Bangkok. She attended Panapan Kindergarten, and Chitralada School for primary and secondary education, where she served as a president of Thai language club. By taking her science program in high school, mathematics piqued her interest in the field of engineering. Started in 2005, she undertook Bachelor of Engineering course in Chemical Engineering at Chulalongkorn University and eventually graduated in 2009. Since her graduation, Jantawan has already worked in many functions. She started off as a procurement officer in Bangkok Synthetics Company Limited, then moved to PTT Chemical Public Company Limited as a Production Information Processing engineer. In an attempt to find more challenging task, she is now working as a process engineer. To take the challenge further, she decided to undertake a Master's degree in Chemical Engineering at Chulalongkorn University, where she studied in the field of Computational Process Engineering. Her graduation is expected to be around December in 2014.